

Exact sensitivity matrix and influence of the number of pilot points in the geostatistical inversion of moment equations of groundwater flow

Monica Riva,¹ Alberto Guadagnini,¹ Francesca De Gaspari,^{1,2,3} and Andres Alcolea^{4,5}

Received 3 August 2009; revised 12 July 2010; accepted 21 July 2010; published 4 November 2010.

[1] We present novel equations for the exact sensitivity matrix of the (ensemble) mean hydraulic head under steady state groundwater flow conditions. These equations are embedded in a geostatistical inverse procedure to condition approximations of stochastic moment equations of flow on measured hydraulic conductivities and heads. Our formulation allows considerable improvement of the methodology proposed by Hernandez et al. (2003, 2006) and renders the inversion of moment equations feasible for a large number of unknown hydraulic parameters. The spatial distribution of the natural logarithm, Y , of conductivity is parameterized within the pilot points framework. Whereas prior values of Y at pilot points are obtained by a variant of kriging, posterior estimates at pilot points are obtained through a maximum likelihood fit of computed to measured heads. The maximum likelihood function also includes a regularization term. By means of a synthetic example and upon adopting formal model information criteria we explore the influence of (1) the number of pilot points and (2) the order of approximation of the governing mean flow equation on our ability to properly estimate the log conductivity and head fields and identify the relative weight of the regularization term and the parameters of the underlying Y variogram. We find that none of the adopted information criteria can identify the optimum number of pilot points and the plausibility weight and variogram parameters values can be determined by the Kashyap's Bayesian measure.

Citation: Riva, M., A. Guadagnini, F. De Gaspari, and A. Alcolea (2010), Exact sensitivity matrix and influence of the number of pilot points in the geostatistical inversion of moment equations of groundwater flow, *Water Resour. Res.*, 46, W11513, doi:10.1029/2009WR008476.

1. Introduction

[2] Predictions of groundwater flow in porous media are typically affected by different sources of uncertainty, including, for example, measurement and parameter uncertainties. These, together with uncertainties in forcing terms, are conveniently tackled upon casting the governing equations in a stochastic framework [e.g., *Dagan and Neuman*, 1997]. In this context, different methods have been developed to condition hydrogeological models not only on direct measurements of parameters but also on measurements of state variables. Linearized stochastic inverse solutions based on cokriging were developed for steady state flow [*Dagan*, 1985; *Hoeksema and Kitanidis*, 1984; *Gutjahr and Wilson*, 1989; *Rubin and Dagan*, 1987]. As demonstrated

by *Zimmerman et al.* [1998], these methods yield reliable parameter estimates for moderate spatial variability but relatively poor estimates and unduly small estimation variances when variability or nonlinearity is pronounced. *Woodbury and Ulrych* [2000] introduced a linearized Bayesian geostatistical inverse approach coupled with a maximum entropy principle that resolves log transmissivity variations on a finite element grid, resulting in improved ability to deal with strongly heterogeneous media [*Jiang et al.*, 2004]. An alternative methodology is offered by Monte Carlo approaches [e.g., *Sahuquillo et al.*, 1992; *LaVenue et al.*, 1995; *RamaRao et al.*, 1995; *Capilla et al.*, 1997; *Gómez-Hernández et al.*, 1997; *Oliver et al.*, 1997; *Hanna and Yeh*, 1998; *Hendricks Franssen and Gómez-Hernández*, 2002; *Alcolea et al.*, 2006b]. These require the generation of a (potentially) large set of random inverse solutions that honor measurements. This may consume a large amount of computer time. Applying them to only a few realizations, as has been the practice to date, may yield plausible representations of reality which however are random and therefore nonunique.

[3] Recently, *Hernandez et al.* [2003, 2006] formulated a nonlinear methodology for the inversion of steady state (ensemble) moment equations of groundwater flow. Log conductivity, Y , is parameterized geostatistically from measured values at discrete locations and unknown values at discrete "pilot points" [*de Marsily*, 1978]. Whereas prior values of Y at pilot points are obtained by a variant of kriging,

¹Dipartimento Ingegneria Idraulica, Ambientale, Infrastrutture Viarie, e Rilevamento, Politecnico di Milano, Milan, Italy.

²Now at GHS, Department of Geotechnical Engineering and Geosciences, Universitat Politècnica de Catalunya, UPC-Barcelona Tech, Barcelona, Spain.

³Also at IDAEA, CSIC, Barcelona, Spain.

⁴Centre of Hydrogeology and Geothermics, University of Neuchâtel, Neuchâtel, Switzerland.

⁵Now at TK Consult AG, Zürich, Switzerland.

posterior estimates at pilot points are obtained through a maximum likelihood fit of computed to measured heads. Optionally, the maximum likelihood function may include a regularization term reflecting prior information on Y ; that is, prior measurements/estimates of parameters and associated errors/uncertainties. Additionally, this term helps to alleviate instability problems due to overparameterization [Tikhonov, 1963a, 1963b; Neuman, 1973; Carrera and Neuman, 1986a; Cooley, 2000; Medina and Carrera, 2003; Alcolea et al., 2006a]. The approach of Hernandez et al. [2003, 2006] provides predictions of hydraulic head and flux through their conditional first moments. Their computational algorithm is based on the recursive finite element approximations of conditional mean flow equations of Guadagnini and Neuman [1999a] and allows rendering either a zero- or a second-order approximation of the mean flow equation (in terms of the standard deviation of Y , σ_Y). Variances of hydraulic head (and flux) are then calculated a posteriori upon solving the corresponding equations. Recently, Hendricks Franssen et al. [2009] compared the relative performance of this moment equations–based inverse method and several types of Monte Carlo and semianalytical inverse methodologies. The methods were assessed in terms of their ability to characterize the log conductivity and head fields and to predict the extent of a well catchment, for mildly and strongly heterogeneous synthetic Y fields. The main conclusions were that observed differences between the performances of the tested methods were not very large. Yet, Monte Carlo inversion of 500 realizations of the particular setup considered needed considerably more CPU time than geostatistical inversion of moment equations.

[4] In spite of the aforementioned advantages, the inversion of moment equations is still based on an optimization process which requires the numerical calculation of the derivatives of the objective function with respect to model parameters. These are calculated from the corresponding derivatives of nodal heads (i.e., the sensitivity matrix). This currently limits the applicability of the method to situations where the number of parameters (e.g., Y values at pilot points) is not large because of the relevant computational cost for calculating the sensitivity matrix at each iteration along the optimization process. We recall that pilot points are introduced to parameterize the underlying Y field by means of a kriging analog. In general, the quality of the fit between calculated and measured heads tends to increase with the number of adjustable parameters (i.e., pilot points). However, the number of parameters can become so large to allow fitting the model to noise, thus causing the quality of the parameter estimates to start deteriorating [Neuman, 1973]. In the context of studies based on the inversion of traditional deterministic flow equations [e.g., de Marsily et al., 1984; RamaRao et al., 1995; Gómez-Hernández et al., 1997; LaVenue and de Marsily, 2001], experience has suggested to locate pilot points on a pseudoregular grid, with spacing of the order of two to three pilot points per correlation range. Using this rule of thumb in practical applications might lead to a very large number of pilot points, with the risk of overfitting [Christensen and Doherty, 2008]. Alcolea et al. [2006a] suggest instead using a minimum of four–five pilot points per correlation range in the context of the Regularized Pilot Points Method. A comprehensive analysis of the effect of the number of pilot points and of the plausibility weight

on the performance of the inversion of groundwater flow moment equations has never been performed.

[5] Here, we start by deriving the equations satisfied by the sensitivity matrix of the (ensemble) mean hydraulic head, up to its second-order approximation. This allows rendering the nonlinear inversion of stochastic moment equations feasible for a large number of unknown parameters. We then explore, on the basis of a synthetic example, the influence of (1) the order of approximation (zero- or second-order) of the governing mean flow equation and (2) the number of pilot points on our ability to properly reconstruct the log conductivity field and to identify the statistical parameters of the underlying variogram of Y , the plausibility weight and the uncertainty associated with the available measurements. Estimation of statistical parameters characterizing the geostatistical model defining the spatial variability of the system is performed on the basis of formal model information/discrimination criteria.

2. Theoretical Background

[6] We consider steady state flow in a randomly heterogeneous porous medium. Guadagnini and Neuman [1999a, 1999b] show how to calculate optimum unbiased predictions of hydraulic head, $h(\mathbf{x})$, via its first statistical moment (the ensemble mean), $\langle h(\mathbf{x}) \rangle_c$, eventually conditioned on measurements of hydraulic conductivity, $K(\mathbf{x})$. The predictor, $\langle h(\mathbf{x}) \rangle_c$, and its associated prediction variance, $\sigma_h^2(\mathbf{x})$, satisfy exact nonlocal integrodifferential equations [Neuman and Orr, 1993]. Guadagnini and Neuman [1999a] render these nonlocal equations workable upon approximating them recursively through expansion in powers of σ_Y , a measure of the (conditional) standard deviation of (natural) log conductivity, $Y(\mathbf{x}) = \ln K(\mathbf{x})$, and develop recursive computational algorithms to solve these equations by Galerkin finite elements up to second order in σ_Y in the presence of measured values of Y . It has then been shown that, when compared to numerical Monte Carlo simulations, second-order approximations of the moment equations yield highly accurate (numerical and/or analytical) solutions for groundwater flows in heterogeneous media with unconditional variance of Y as large as 4 and different ratios between a characteristic length scale characterizing the geometry of the domain and the correlation scale of the Y field [e.g., Guadagnini and Neuman, 1999a; Riva et al., 2001; Guadagnini et al., 2003]. We report in Appendix A the finite element equations of Guadagnini and Neuman [1999a] in the presence of deterministic sources and boundary conditions. These constitute the starting point for the development of the exact sensitivity matrix presented in section 4. We have embedded the inversion of the flow moment equations by means of the evaluation of the exact sensitivity matrix in a new numerical code (inverse moment equations (INME)), which extends the earlier code of Guadagnini and Neuman [1999b] by also handling irregular domain shapes, rectangular and triangular elements, and general deterministic boundary conditions.

[7] As shown in Appendix A, the solution of the zero- and second-order approximations of the mean flow equations and its associated (co)variance requires the knowledge of (1) the mean geometric hydraulic conductivity, $K_C(\mathbf{x}) = \exp(\langle Y(\mathbf{x}) \rangle_c)$, and (2) the conditional covariance of the Y field, $C_{Yc}(\mathbf{x}, \mathbf{y}) = \langle Y(\mathbf{x}) Y(\mathbf{y}) \rangle_c$, between points \mathbf{x} and \mathbf{y} .

Hernandez et al. [2003, 2006] developed a nonlinear geostatistical inverse procedure on the basis of a maximum likelihood approach (ML) to condition $\langle Y(\mathbf{x}) \rangle_c$ and $C_{Yc}(\mathbf{x}, \mathbf{y})$ on measured values of Y and h . Estimation of $\langle Y(\mathbf{x}) \rangle_c$ is performed upon parameterizing it as a weighted sum of N_M values $Y_{Mi}(\mathbf{x}_i)$ at discrete measurement points \mathbf{x}_i ($i = 1, \dots, N_M$), if available, and N_P values $Y_{Pj}(\mathbf{x}_j)$ ($j = 1, \dots, N_P$) at discrete pilot point locations [de Marsily, 1978; de Marsily et al., 1984].

$$\langle Y(\mathbf{x}) \rangle_c = \sum_{i=1}^{N_M} \lambda_i(\mathbf{x}) Y_{Mi}(\mathbf{x}_i) + \sum_{j=1}^{N_P} \lambda_j(\mathbf{x}) Y_{Pj}(\mathbf{x}_j) = \sum_{k=1}^{N_Y} \lambda_k(\mathbf{x}) Y_{Hk}(\mathbf{x}_k) \quad (1)$$

Here, $N_Y = N_M + N_P$, $\lambda_i(\mathbf{x})$ and $\lambda_j(\mathbf{x})$ (and so $\lambda_k(\mathbf{x})$) are ordinary kriging weights to be determined, Y_{Hk} is the k component of the vector of hydraulic parameters $\mathbf{Y}_H = (\mathbf{Y}_M, \mathbf{Y}_P)^T$, \mathbf{Y}_M and \mathbf{Y}_P being vectors formed by values of Y_{Mi} and Y_{Pj} , respectively. The values of $Y_{Mi}(\mathbf{x}_i)$ and $Y_{Pj}(\mathbf{x}_j)$ (the first optionally if measurements of Y affected by errors are available) are estimated by inversion in a ML framework (see below for details). Pilot points are introduced to parameterize $\langle Y(\mathbf{x}) \rangle_c$ by means of a kriging analog. The identification of the optimum number of pilot points is an important task of this investigation. We assume that $Y(\mathbf{x})$ has statistically homogeneous spatial increments or fluctuations about a spatial drift of known form (e.g., polynomial, logarithmic, or based on surrogate data such as rock/soil type or petrophysical/pedological characteristics) but unknown coefficients. In either case, the spatial structure of $Y(\mathbf{x})$ is characterized by a variogram function $\gamma(\mathbf{s}; \boldsymbol{\theta})$ where \mathbf{s} is a lag vector and $\boldsymbol{\theta}$ a vector of variogram parameters. Here, we consider a single (i.e., nonnested) variogram structure characterized by sill (σ_Y^2) and integral scale (I_Y). Yet, more sophisticated variograms including, for example, anisotropy, can be accommodated in the approach. If there is a sufficiently large number of reliable measurements of Y , $\boldsymbol{\theta}$ can be estimated directly from these data [e.g., Samper and Neuman, 1989a, 1989b]. Here, we explore the possibility of estimating $\boldsymbol{\theta}$ within the context of the optimization process by means of suitable model information/discrimination criteria to render it fully conditional on available measurements [e.g., Hernandez et al., 2006, and references therein]. Having an estimate of $\boldsymbol{\theta}$, a prior estimate of Y at pilot points together with the corresponding prior estimation variance-covariance can be obtained by standard methods (e.g., variants of kriging; see Deutsch and Journel [1998]). Estimation of Y at measurement and pilot point locations during inversion is based on N_M measurements of Y and N_h measurements of h .

[8] We set

$$Y_{Mi}^* = Y_{Mi} + \varepsilon_{Yi}^* \quad i = 1, \dots, N_M \quad (2)$$

$$h_j^* = h_j + \varepsilon_{hj}^* \quad j = 1, \dots, N_h \quad (3)$$

where Y_{Mi} and h_j are the unknown true values of Y and h at measurement points \mathbf{x}_i and \mathbf{x}_j , respectively, Y_{Mi}^* and h_j^* their measured values and ε_{Yi}^* and ε_{hj}^* are zero-mean uncorrelated measurement errors. Following the work of Carrera and Neuman [1986a], we assume that the measurement errors of Y and h (1) lack correlation and (2) are

multivariate Gaussian. In addition, the covariance matrices of measurements errors, \mathbf{C}_h for heads and \mathbf{C}_{YM} for log conductivity,

$$\mathbf{C}_h = \sigma_{hE}^2 \mathbf{V}_h; \quad \mathbf{C}_{YM} = \sigma_{YE}^2 \mathbf{V}_{YM} \quad (4)$$

are unknown up to the positive scalars σ_{hE}^2 and σ_{YE}^2 (these quantities are typically unknown and can be estimated during inversion, as detailed in what follows) and ε_{Yi}^* and ε_{hj}^* are not correlated in space (it then follows that the matrices \mathbf{V}_h and \mathbf{V}_{YM} are diagonal). Note that \mathbf{V}_{YM} reflects measurement uncertainties of Y only (i.e., it does not include any source of parameter uncertainty).

[9] The ML estimate of $\langle Y(\mathbf{x}) \rangle_c$ is obtained by minimizing the following function (negative log likelihood criterion; see Carrera and Neuman [1986a]) with respect to model parameters

$$NLL = \frac{F_h}{\sigma_{hE}^2} + \frac{F_Y}{\sigma_{YE}^2} + \ln|\mathbf{V}_Y| + \ln|\mathbf{V}_h| + N_h \ln \sigma_{hE}^2 + N_Y \ln \sigma_{YE}^2 + N_z \ln 2\pi \quad (5)$$

Here, N_z is the total number of measurements ($N_z = N_h + N_Y$) and the covariance matrix of the vector of measurement errors, $\boldsymbol{\varepsilon}_Y^*$, is written as

$$\mathbf{C}_Y = \begin{bmatrix} \mathbf{C}_{YM} & \mathbf{0} \\ \mathbf{0} & \mathbf{C}_{YP} \end{bmatrix} = \sigma_{YE}^2 \mathbf{V}_Y = \sigma_{YE}^2 \begin{bmatrix} \mathbf{V}_{YM} & \mathbf{0} \\ \mathbf{0} & \mathbf{V}_{YP} \end{bmatrix} \quad (6)$$

where \mathbf{C}_Y is formed by the diagonal covariance matrix of Y measurements errors, \mathbf{C}_{YM} , and the nondiagonal symmetric covariance matrix of Y estimation errors at pilot points, $\mathbf{C}_{YP} = \sigma_{YE}^2 \mathbf{V}_{YP}$. Whereas \mathbf{V}_h and \mathbf{V}_{YM} are fixed, \mathbf{V}_{YP} is a function of the variogram parameters $\boldsymbol{\theta}$. As such, \mathbf{V}_{YP} is updated during the inversion process. Note that full correlation is included during the inverse process. As a result, the variance of pilot points located close to measurement points will be small. The quantity F_h in (5) is the head residual criterion (also termed objective function of heads)

$$F_h = \left(\mathbf{h}^* - \langle \mathbf{h}^{[a]} \rangle_c \right)^T \mathbf{V}_h^{-1} \left(\mathbf{h}^* - \langle \mathbf{h}^{[a]} \rangle_c \right) \quad (7)$$

where superscript T denotes transpose, \mathbf{h}^* is the vector of head measurements, $\langle \mathbf{h}^{[a]} \rangle_c$ is a vector of a -order mean conditional hydraulic head values (i.e., $a = 0$ or 2, depending on the order of approximation of $\langle \mathbf{h} \rangle_c$ evaluated according to equations (A1)–(A7) at head measurement locations. F_Y is the penalty parameter criterion (also termed objective function of parameters)

$$F_Y = \left(\mathbf{Y}^* - \langle \mathbf{Y} \rangle_c \right)^T \mathbf{V}_Y^{-1} \left(\mathbf{Y}^* - \langle \mathbf{Y} \rangle_c \right) \quad (8)$$

where \mathbf{Y}^* is the vector of Y measurements and Y prior estimates at pilot point locations, $\langle \mathbf{Y} \rangle_c$ is a vector of mean Y values evaluated during inversion (performed at order a) at Y measurement and pilot point locations. Calculating $\langle \mathbf{h}^{[a]} \rangle_c$ at each iteration during the optimization process entails having at our disposal the current estimates of $\langle Y(\mathbf{x}) \rangle_c$ (for $a = 0$), $\langle Y^2(\mathbf{x}) \rangle_c$ and $\langle Y'(\mathbf{x}) Y'(\mathbf{y}) \rangle_c$ (for $a = 2$). This is achieved by estimating Y at measurements and pilot point locations through minimization of (5) and projecting these estimates on the computational grid by posterior kriging.

Following *Guadagnini and Neuman* [1999a], we treat mean log conductivity as constant at each element and approximate the covariance $\langle Y'(\mathbf{x}) Y'(\mathbf{y}) \rangle_c$ between any point \mathbf{x} in element e and \mathbf{y} in element e' by $\langle Y'(\mathbf{x}^e) Y'(\mathbf{y}^{e'}) \rangle_c \equiv \langle Y'(e) Y'(e') \rangle_c$, where \mathbf{x}^e and $\mathbf{y}^{e'}$ are the centroids of elements e and e' (see Appendix A for details). *Hernandez et al.* [2006] derived the following equation for the posterior covariance of Y (solved at each iteration of the optimization process)

$$\begin{aligned} \langle Y'(\mathbf{x}) Y'(\mathbf{y}) \rangle_c &= \langle [Y(\mathbf{x}) - \langle Y(\mathbf{x}) \rangle_c] [Y(\mathbf{y}) - \langle Y(\mathbf{y}) \rangle_c] \rangle_c \\ &= \left\langle \left[Y(\mathbf{x}) - \sum_{k=1}^{N_Y} \lambda_k(\mathbf{x}) Y_{Hk} \right] \left[Y(\mathbf{y}) - \sum_{i=1}^{N_Y} \lambda_i(\mathbf{y}) Y_{Hi} \right] \right\rangle_c \\ &= -\gamma(\mathbf{x} - \mathbf{y}, \boldsymbol{\theta}) - \sum_{k=1}^{N_Y} \lambda_k(\mathbf{x}) \sum_{i=1}^{N_Y} \lambda_i(\mathbf{y}) [\gamma(\mathbf{x}_k - \mathbf{x}_i, \boldsymbol{\theta}) - Q_{ki}] \\ &\quad + \sum_{i=1}^{N_Y} \lambda_i(\mathbf{x}) \gamma(\mathbf{x} - \mathbf{x}_i, \boldsymbol{\theta}) + \sum_{i=1}^{N_Y} \lambda_i(\mathbf{y}) \gamma(\mathbf{y} - \mathbf{x}_i, \boldsymbol{\theta}) \end{aligned} \quad (9)$$

Here, Q_{ki} are components of the parameter estimation covariance matrix $\mathbf{Q} \equiv \langle (\mathbf{Y} - \langle \mathbf{Y}_H \rangle_c) (\mathbf{Y} - \langle \mathbf{Y}_H \rangle_c)^T \rangle$. The posterior variance of Y is obtained by (9) upon setting $\mathbf{x} = \mathbf{y}$.

3. Optimization Procedure and Role of Model Discrimination Criteria

[10] Minimization of (5) with respect to Y_{Hj} (with $j = 1, \dots, N_Y$), σ_{hE}^2 , σ_{yE}^2 and variogram parameters (included in vector $\boldsymbol{\theta}$) is not a trivial task and might lead to unstable results [*Carrera and Neuman*, 1986a, 1986b]. We follow *Carrera and Neuman* [1986a, 1986c] and *Hernandez et al.* [2006] and minimize (5) with respect to \mathbf{Y}_H for selected values of $\boldsymbol{\theta}$, σ_{hE}^2 and σ_{yE}^2 . We then improve upon these values as described below and repeat the process iteratively until convergence is attained. When $\boldsymbol{\theta}$, σ_{hE}^2 and σ_{yE}^2 are set, minimization of (5) reduces to the minimization of

$$F = F_h + \mu F_Y \quad (10)$$

where μ is the plausibility weight

$$\mu = \frac{\sigma_{hE}^2}{\sigma_{yE}^2} \quad (11)$$

For given $\boldsymbol{\theta}$ and μ we minimize (10) using the iterative Levenberg-Marquardt algorithm, which we implement within the code INME. The minimization algorithm computes an updated parameter estimate $\hat{\mathbf{Y}}_H$ of the (unknown) true vector \mathbf{Y} and a Cramer-Rao lower bound approximation for the covariance matrix of the corresponding estimation errors. The latter is evaluated according to $\mathbf{Q} = \sigma_{hE}^2 [\mathbf{J}^T \mathbf{V}_h^{-1} \mathbf{J} + \mu \mathbf{V}_Y^{-1}]^{-1}$ where \mathbf{J} is the Jacobian matrix of (ensemble mean) head derivatives with respect to \mathbf{Y} , evaluated at $\hat{\mathbf{Y}}_H$. Next, $\hat{\mathbf{Y}}_H$ is projected onto the finite element grid via the posterior kriging algorithm described above. This allows solving the finite element equations for updated conditional mean head values, providing the next iteration with starting data. The iterative process continues until one of the following criteria is met: (1) the gradient norm is very small ($\|\nabla F\| \leq 10^{-5}$), (2) the ratio between the gradient norm and its value at the first iteration is small enough ($\|\nabla F\|/\|\nabla F\|_1 \leq 10^{-5}$) or (3) the maximum increment of parameters between two consecutive

iterations is very small ($< 10^{-4}$). The second condition is usually considered the best criterion of convergence [e.g., *Carrera and Neuman*, 1986c; *Alcolea et al.*, 2006a]. Following convergence of the minimization process, estimates of $Y(\mathbf{x})$, rendered by (1) at elements centroids, and corresponding variance-covariance computed according to (9) are fully conditioned on all available data (log conductivity and/or heads). The results depend on the order (zero- or second-order) of approximation adopted for the (mean) flow equation. This will be further explored in section 5.

[11] We note that, while the analysis of *Hernandez et al.* [2006] was limited to a fixed and known value of the plausibility weight ($\mu = 1$), minimization of (10) should be performed for a sequence of μ and $\boldsymbol{\theta}$ values. *Carrera and Neuman* [1986a] suggest that, when μ is unknown, the optimum value of μ should be the one leading to a minimum value of NLL in (5). In section 5 we explore the ability of NLL and the following model information/discrimination criteria

$$\begin{aligned} AIC &= NLL + 2N_Y; \quad AIC_c = AIC + \frac{2N_Y(N_Y + 2)}{N_h - 1}; \\ BIC &= NLL + N_Y \ln N_Z; \quad HIC = NLL + 2N_Y \ln(\ln N_Z); \\ KIC &= NLL + N_Y \ln\left(\frac{N_Z}{2\pi}\right) - \ln|\mathbf{Q}| \end{aligned} \quad (12)$$

to identify the optimum value of μ in the context of inversion of mean groundwater flow at different orders of approximation. In (12), AIC is due to *Akaike* [1974], BIC to *Schwarz* [1978], HIC to *Hannan* [1980], KIC to *Kashyap* [1982] and AICc is presented by *Hurvich and Tsai* [1989].

[12] We follow this by ML estimate of σ_{hE}^2 and σ_{yE}^2 according to [*Carrera and Neuman*, 1986a]

$$\sigma_{hE}^2 = \frac{F_{\min}}{N_Z}; \quad \sigma_{yE}^2 = \frac{\sigma_{hE}^2}{\mu} \quad (13)$$

where F_{\min} is the value of F (10) at the end of the optimization procedure. We repeat the evaluation of μ , σ_{hE}^2 and σ_{yE}^2 for a sequence of discrete values of $\boldsymbol{\theta}$, interpreting each as representative of a different model, depicting a different heterogeneous spatial distribution of log conductivity, along the lines of *Hernandez et al.* [2006]. We select an optimum value of $\boldsymbol{\theta}$ on the basis of how sharply it corresponds to a minimum of any of the selected model information criteria.

[13] Model discrimination criteria can be used a posteriori (after inversion) in order to propose a selection among a set of candidate models. In principle, one could use such criteria to select the number of hydraulic parameters to be estimated during inversion (e.g., the optimum number of pilot points), the order of approximation (zero- or second-order) adopted for the equation governing the mean groundwater flow, and the functional form of the log conductivity variogram. All these discrimination criteria support the principle of parsimony, in that, when everything else is equal, the model with the smallest number of parameters is preferable. If the number of parameters and observation data is fixed, minimization of any of the quantities in (12), with the only exception of KIC, is equivalent to minimizing NLL. KIC is the only discrimination criterion that, by means of $|\mathbf{Q}|$, balances parsimony with the expected information content. In other words, KIC is unique to favor models with smaller

expected information content per observation [see also *Ye et al.*, 2008].

4. Derivation of the Sensitivity Matrix for Mean Heads

[14] As stated in section 3, we minimize (10) using the iterative Levenberg-Marquardt's algorithm. This second-order optimization method belongs to the Gauss-Newton family and often requires a small number of iterations to converge [*Marquardt*, 1963; *Nowak and Cirpka*, 2004; *Carrera et al.*, 2005]. However, it requires the evaluation of the sensitivity matrix; that is, the derivatives of heads at nodal points with respect to model parameters. These derivatives can be calculated in several ways. A common procedure consists in approximating the derivatives by the incremental ratio (finite differences approximation). This methodology is adopted in widely used external optimization packages (e.g., PEST; see *Doherty* [2002]). It allows evaluating the derivatives using model-generated observations calculated on the basis of incrementally varied parameter values. Then, it involves the solution of the forward problem as many times as (or twice) the number of the parameters when a forward (or a central) finite difference scheme is adopted to approximate the derivatives. Yet, the simplicity comes at the cost of large CPU times. A finite difference scheme becomes computationally demanding as the number of parameters increases and limits the degrees of freedom for reproducing the variability of hydraulic properties. In the context of groundwater flow moment equations, *Hernandez et al.* [2003, 2006] approximate the derivatives of heads with respect to model parameters by the central finite differences method to obtain an adequate solution of the inverse problem. As such, their procedure becomes computationally not appealing for a large number of parameters (N_Y). As an alternative, one can directly solve the system of equations governing the derivatives. This methodology has not been developed until now, owing to the formal complexity of the moment equations. Its key advantages are: (1) it provides the exact solution for the derivatives, thus increasing the accuracy of the inversion procedure; (2) the equations to be solved are N_Y (and not $2N_Y$ as in the central finite differences scheme); and (3) the system matrices are identical for all the parameters and coincide with those used to solve the forward problem (see sections 4.1 and 4.2), thus ultimately leading to a drastic reduction of the total CPU time.

[15] The derivative of the second-order approximation of the mean conditional head, $\langle h^{[2]} \rangle_c$, with respect to the j th hydraulic parameter Y_{H_j} ($j = 1, \dots, N_Y$) is given by

$$\frac{\partial \langle h^{[2]} \rangle_c}{\partial Y_{H_j}} = \frac{\partial \langle h^{(0)} \rangle_c}{\partial Y_{H_j}} + \frac{\partial \langle h^{(2)} \rangle_c}{\partial Y_{H_j}} \quad (14)$$

$\langle h^{(0)} \rangle_c$ and $\langle h^{(2)} \rangle_c$ being the zero- and second-order component of mean hydraulic heads, respectively. In sections 4.1 and 4.2 we develop novel equations satisfied by the terms included in (14). These equations have been implemented in the code INME.

4.1. Zero-Order Component

[16] The zero-order component of the hydraulic head in (14) coincides with the solution of the traditional deterministic flow equation in an aquifer with local hydraulic

conductivity equal to the mean geometric hydraulic conductivity, $K_G(\mathbf{x})$. This can clearly be seen from (A1) (see also *Neuman and Guadagnini* [1999] for an extensive discussion). If the mean forcing term is not a function of Y_{H_j} (as is often the case), derivation of (A1) with respect to Y_{H_j} leads to

$$\sum_{m=1}^N A_{nm} \frac{\partial h_m^{(0)}}{\partial Y_{H_j}} = - \sum_{m=1}^N \frac{\partial A_{nm}}{\partial Y_{H_j}} h_m^{(0)}; n = 1, \dots, N \quad (15)$$

where $h_m^{(0)} \equiv \langle h^{(0)}(\mathbf{x}_m) \rangle_c$ is the zero-order approximation of the mean hydraulic head at grid node m , N is the number of nodes defining the finite element mesh, excluding those at Dirichlet boundaries, and A_{nm} are terms of a sparse symmetric matrix given by (A2). The derivative of A_{nm} with respect to Y_{H_j} can be obtained from (A2) as

$$\frac{\partial A_{nm}}{\partial Y_{H_j}} = \int_{\Omega} \exp \langle Y(\mathbf{x}) \rangle_c \frac{\partial \langle Y(\mathbf{x}) \rangle_c}{\partial Y_{H_j}} \nabla \psi_n \cdot \nabla \psi_m d\mathbf{x} \quad (16)$$

Here, Ω is the flow domain, ψ_n and ψ_m being basis functions (see Appendix A for further details). Derivation of (1) with respect to Y_{H_j} leads to

$$\frac{\partial \langle Y(\mathbf{x}) \rangle_c}{\partial Y_{H_j}} = \lambda_j(\mathbf{x}) \quad (17)$$

Then, making use of (16) and (17), (15) becomes

$$\sum_{m=1}^N A_{nm} \frac{\partial h_m^{(0)}}{\partial Y_{H_j}} = - \sum_{m=1}^N h_m^{(0)} \int_{\Omega} \exp \langle Y(\mathbf{x}) \rangle_c \lambda_j(\mathbf{x}) \nabla \psi_n \cdot \nabla \psi_m d\mathbf{x}; n = 1, \dots, N \quad (18)$$

Note that all the terms required to evaluate $\partial h_m^{(0)} / \partial Y_{H_j}$ are calculated during the forward solution of the equation satisfied by $\langle h_m^{(0)} \rangle_c$.

4.2. Second-Order Component

[17] Derivation of (A3) with respect to Y_{H_j} leads to

$$\begin{aligned} \sum_{m=1}^N A_{nm} \frac{\partial h_m^{(2)}}{\partial Y_{H_j}} &= \frac{\partial P_n}{\partial Y_{H_j}} + \frac{\partial S_n}{\partial Y_{H_j}} - \sum_{m=1}^N h_m^{(2)} \frac{\partial A_{nm}}{\partial Y_{H_j}} \\ &\quad - \sum_{m=1}^N h_m^{(0)} \frac{\partial B_{nm}}{\partial Y_{H_j}} - \sum_{m=1}^N B_{nm} \frac{\partial h_m^{(0)}}{\partial Y_{H_j}}; n = 1, \dots, N; \end{aligned} \quad (19)$$

where $h_m^{(2)} \equiv \langle h^{(2)}(\mathbf{x}_m) \rangle_c$ is the second-order component of the mean hydraulic head at grid node m and all remaining symbols are introduced in Appendix A. We start by noting that the posterior covariance of Y defined by (9) does not depend on Y_{H_j} . This follows by noting that deriving (9) with respect to Y_{H_j} and recalling the unbiased condition yields

$$\begin{aligned} \frac{\partial}{\partial Y_{H_j}} \langle Y'(\mathbf{x}) Y'(\mathbf{y}) \rangle &= -\lambda_j(\mathbf{x}) \left[\langle Y(\mathbf{y}) \rangle - \sum_{i=1}^{N_Y} \lambda_i(\mathbf{y}) \langle Y_{Hi} \rangle \right] \\ &\quad - \lambda_j(\mathbf{y}) \left[\langle Y(\mathbf{x}) \rangle - \sum_{k=1}^{N_Y} \lambda_k(\mathbf{x}) \langle Y_{Hk} \rangle \right] = 0 \end{aligned} \quad (20)$$

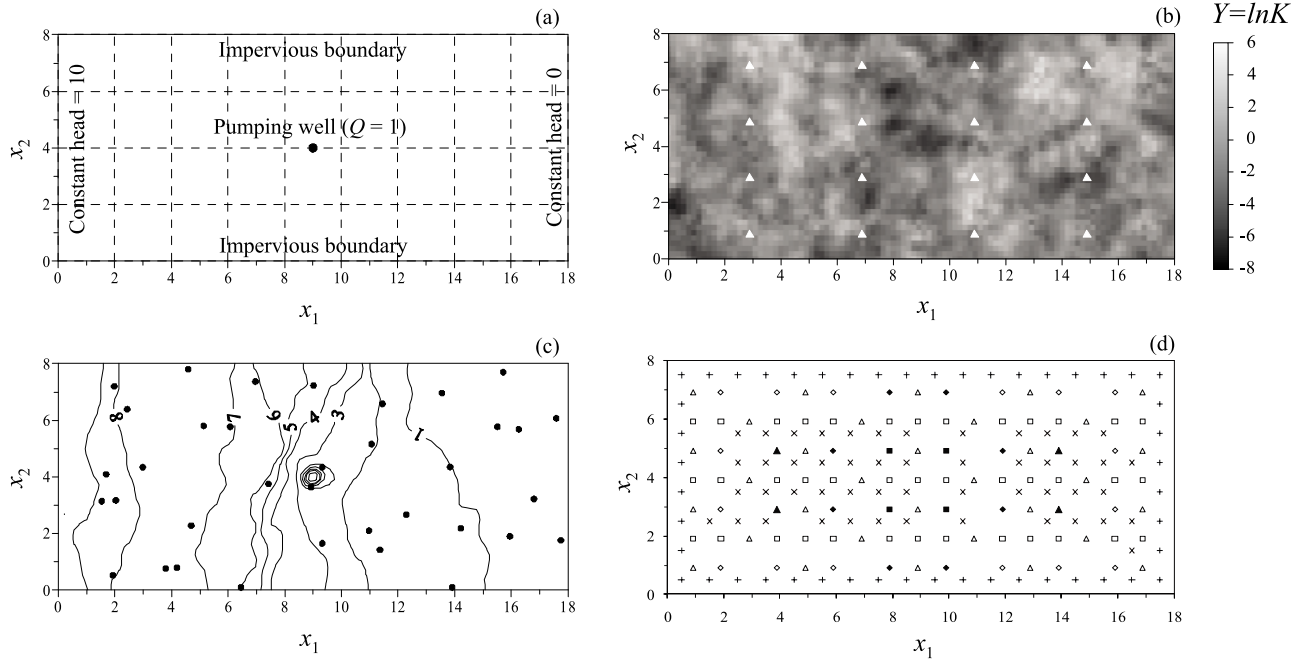


Figure 1. (a) Setup of the groundwater flow test problem. (b) The Y reference field; Y measurement locations are depicted by triangles. (c) The h reference field; h measurement locations are depicted by dots. (d) The pilot point locations: $N_p = 4$ (solid square), $N_p = 8$ (solid square and solid triangle), $N_p = 16$ (solid square, solid triangle, and solid diamond), $N_p = 32$ (solid square, solid triangle, solid diamond, and open diamond), $N_p = 64$ (solid square, solid triangle, solid diamond, open diamond, and open triangle), $N_p = 103$ (solid square, solid triangle, solid diamond, open diamond, open triangle, and open square), $N_p = 150$ (solid square, solid triangle, solid diamond, open diamond, open triangle, open square, and plus), $N_p = 200$ (solid square, solid triangle, solid diamond, open diamond, open triangle, open square, plus, and cross).

The derivative of P_n with respect to Y_{H_j} in (19) is obtained from (A6) as

$$\frac{\partial P_n}{\partial Y_{H_j}} = - \sum_{m=1}^{N_D} \left[h_m^{(2)} \frac{\partial A_{nm}}{\partial Y_{H_j}} + A_{nm} \frac{\partial h_m^{(2)}}{\partial Y_{H_j}} + h_m^{(0)} \frac{\partial B_{nm}}{\partial Y_{H_j}} + B_{nm} \frac{\partial h_m^{(0)}}{\partial Y_{H_j}} \right] \quad (21)$$

where N_D is the number of Dirichlet boundary nodes. The term $\partial B_{nm} / \partial Y_{H_j}$ in (19) and (21) is obtained by (A5) and (17) as

$$\frac{\partial B_{nm}}{\partial Y_{H_j}} = \frac{1}{2} \int_{\Omega} \lambda_l(\mathbf{x}) \langle Y'(\mathbf{x})^2 \rangle_c \exp[\langle Y(\mathbf{x}) \rangle_c] \nabla \psi_n(\mathbf{x}) \cdot \nabla \psi_m(\mathbf{x}) dx \quad (22)$$

The term $\partial S_n / \partial Y_{H_j}$ in (19) is obtained on the basis of (A7) and (17) as

$$\begin{aligned} \frac{\partial S_n}{\partial Y_{H_j}} &= \sum_{e=1}^{M_x} \exp[Y(e)] \sum_{e'=1}^{M_y} \exp[\langle Y(e') \rangle] \langle Y'(e) Y'(e') \rangle_c \\ &\cdot \sum_{i=1}^{N_x} \theta_{ni}^{ee'} \sum_{l=1}^{N_y} \sum_{k=1}^{N_z} \Delta_{lk}^{e'e'} \\ &\cdot \left[(\lambda_j(e) + \lambda_j(e')) G_{il}^{ee'} h_k^{(0)e'} + \frac{\partial G_{il}^{ee'}}{\partial Y_{H_j}} h_k^{(0)e'} + G_{il}^{ee'} \frac{\partial h_k^{(0)e'}}{\partial Y_{H_j}} \right] \end{aligned} \quad (23)$$

where $\lambda_j(e) = \lambda_j(\mathbf{x}^e)$, $\lambda_j(e') = \lambda_j(\mathbf{y}^{e'})$, $G_{il}^{ee'}$ is the Green's function associated with the zero-order mean flow equation (A1) evaluated at node i of element e owing to a unit source at node l of element e' , and all remaining symbols are introduced in Appendix A. The equations satisfied by $G_{il}^{ee'}$ and its derivative are briefly reported in Appendix B (see *Guadagnini and Neuman [1999a]* for additional details). Substituting (21), (22) and (23) in (19) and making use of (B1) and (B3), one can finally evaluate the second-order component of the derivatives of the mean hydraulic head with respect to hydraulic parameters Y_{H_j} . Note that all the terms required to evaluate $\partial \langle h_m^{(2)} \rangle_c / \partial Y_{H_j}$ are calculated during the forward solution of the equation satisfied by $\langle h_m^{(0)} \rangle_c$ and $\langle h_m^{(2)} \rangle_c$.

5. Illustrative Example

[18] We illustrate our methodology by means of a synthetic groundwater flow scenario similar to that analyzed by *Hernandez et al. [2006]*. This allows us to compare the performance and the accuracy of the new algorithm with a scenario taken from the literature as reference. We consider superimposition of mean uniform and convergent flows in a rectangular domain of length 18 and width 8 (all quantities hereinafter are given in consistent units). Figure 1a depicts a sketch of the flow domain, with the type of boundary conditions used. The domain is discretized into $N_e = 3600$ square elements (40 rows \times 90 columns) of uniform size $\delta = 0.2$. Deterministic head values of 10 and 0 are prescribed along the

left and right boundaries, respectively, whereas the top and the bottom boundaries are impervious. A well is located in the center of the domain and pumps continuously at a constant unit rate.

[19] Using a sequential Gaussian simulator (GCOSIM3D; see *Gómez-Hernández and Journel, 1993*) we generate a single unconditional realization of Y with zero mean, exponential isotropic variogram with given sill, $\sigma_Y^2 = 4.0$, and integral scale, $I_Y = 1.0$. We purposefully set the Y variogram sill to a value which is relatively large for a system characterized by a single geological unit in order to test the performance of the methodology. We solve the forward flow problem to obtain the corresponding distribution of heads. These constitute our reference values of hydraulic conductivity (Figure 1b) and heads (Figure 1c). We sample the reference head field at 36 measurements points (depicted by dots in Figure 1c) and the Y field at 16 points (indicated by triangles in Figure 1b). We superimpose a white Gaussian measurement error with unit variance on both sets of measurements ($\sigma_{YE}^2 = \sigma_{hE}^2 = 1.0$; i.e., $\mu = 1.0$ according to (11)) and estimate Y at pilot points by prior ordinary kriging of the noisy Y “measurements.” This renders a percentage error associated with hydraulic head measurements that increases from 10% (close to the left boundary) to more than 100% (near the right boundary, where heads are close to the prescribed zero value), with an average value of about 50%. The average percentage error associated with the Y measurements is about 100%. These uncertainties on available measurements can be quite common in practical situations where only the order of magnitude of hydraulic conductivity is often known (e.g., Y measurements interpreted from particle-size distributions) and head measurements are affected by the accuracy of the instruments, human errors and external factors (e.g., electrical interference and/or variations in atmospheric pressure).

[20] In our analysis we consider eight different networks of 4, 8, 16, 32, 64, 103, 150 and 200 pilot points. Figure 1d reports the details on the number and location of pilot points for each scenario investigated. In sections 5.1 and 5.2 we explore: (1) the benefit of basing the inversion of moment equations on the direct calculation of the derivatives; (2) the effect of the number of pilot points on the reconstruction of the Y and h fields by means of either a zero- and/or a second-order inversion; and (3) the ability of the inversion procedure to estimate not only the Y field but also the plausibility weight μ , the uncertainty associated with available Y and h measurements, and the parameters of the Y variogram, whose functional form is assumed to be known. For these purposes, and according to the methodology described in section 3, we solve the inverse problem for various combinations of (1) values of the plausibility weight ($\mu = 0.01, 0.1, 0.5, 0.75, 1.0, 5, 10, 100$), (2) variogram sill ($\sigma_Y^2 = 0.5, 1.0, 2.0, 3.0, 3.5, 4.0, 4.5, 5.0, 6.0$), and (3) integral scale ($I_Y = 0.25, 0.5, 1.0, 2.0, 4.0$) for each network of pilot points selected. According to the optimization procedure outlined in section 3, this corresponds to estimate the statistical parameters μ , I_Y and σ_Y^2 through an exhaustive search, while the characterization of Y is carried out by traditional (direct) optimization.

[21] We analyze the impact of a complete second-order solution by performing the inversion in two different ways: (1) approximating the mean hydraulic head in (7) by its zero-order component ($a = 0$; we denote this as zero-order

inversion), and (2) computing the complete second-order solution for the mean hydraulic head ($a = 2$ in (7); we denote this as second-order inversion). Overall, about 3000 scenarios (for each order of inversion) have been explored. A summary of the results is presented below. Numerical computations have been performed on a CILEA supercomputer, cluster Xeon-Exadron of 128 two-way nodes with an Intel Xeon 3.06GHz CPU.

5.1. Influence of the Number of Pilot Points and Estimation of the Plausibility Weight and Variogram Parameters

[22] A global quantitative analysis about the quality of the reconstructed Y and h fields can be performed by evaluating the mean absolute error and root-mean-square error of Y ($\bar{\epsilon}_Y$ and $RMSE_Y$, respectively) and h ($\bar{\epsilon}_h$ and $RMSE_h$), defined as

$$\bar{\epsilon}_Y = \frac{1}{N_e} \sum_{i=1}^{N_e} \left| \langle Y(\mathbf{x}_i^e) \rangle_c^{[a]} - Y_{ref}(\mathbf{x}_i^e) \right|;$$

$$RMSE_Y = \sqrt{\frac{1}{N_e} \sum_{i=1}^{N_e} \left[\langle Y(\mathbf{x}_i^e) \rangle_c^{[a]} - Y_{ref}(\mathbf{x}_i^e) \right]^2}, \quad (24)$$

$$\bar{\epsilon}_h = \frac{1}{N_g} \sum_{j=1}^{N_g} \left| \langle h^{[a]}(\mathbf{x}_j) \rangle_c - h_{ref}(\mathbf{x}_j) \right|;$$

$$RMSE_h = \sqrt{\frac{1}{N_g} \sum_{j=1}^{N_g} \left[\langle h^{[a]}(\mathbf{x}_j) \rangle_c - h_{ref}(\mathbf{x}_j) \right]^2} \quad (25)$$

Here, $\langle Y(\mathbf{x}_i^e) \rangle_c^{[a]}$ ($a = 0$ or 2) is the mean Y field estimated during the a -order inversion at the N_e element centroids, \mathbf{x}_i^e ; $Y_{ref}(\mathbf{x}_i^e)$ and $h_{ref}(\mathbf{x}_j^e)$ are error-free reference values of Y and h evaluated at points \mathbf{x}_i^e and \mathbf{x}_j , respectively; \mathbf{x}_j are the coordinates of grid nodes and N_g is the number of nodes (3731 in our example). For comparison purposes, we perform our calculations (1) with the procedure of *Hernandez et al. [2006]*, who couple the solution of the flow problem with the public domain code PEST [*Doherty, 2002*], and (2) with our code INME, which makes full use of the expressions developed in section 4. As an example, Figure 2 depicts the calculated mean absolute error of Y (Figure 2a) and h (Figure 2b) as a function of the number of pilot points and the order of inversion for $\sigma_Y^2 = 4.0$, $I_Y = 1.0$ and $\mu = 1.0$ (i.e., the true, reference values). Figure 2 compares the results obtained by INME (solid lines), on the basis of the expressions presented in section 4, with those obtained following the procedure of *Hernandez et al. [2006]*, who approximate the sensitivity matrix by the incremental ratio (dashed lines). A similar behavior has been observed for the root-mean-square errors (not reported). The CPU time (in hours) required for each second-order inversion is also reported in Figure 2a. Zero-order inversion based on the direct calculation of the sensitivity matrix requires less than one minute for all cases analyzed. When the solution of the flow problem is coupled with PEST, the execution time needed for a zero-order inversion ranges between about half to one third (depending on N_p) of the time required for a second-order inversion. The use of the exact sensitivity matrix results in an improved accuracy of the reconstruction of the Y field, especially when a second-order inversion is performed. Figure 2a suggests

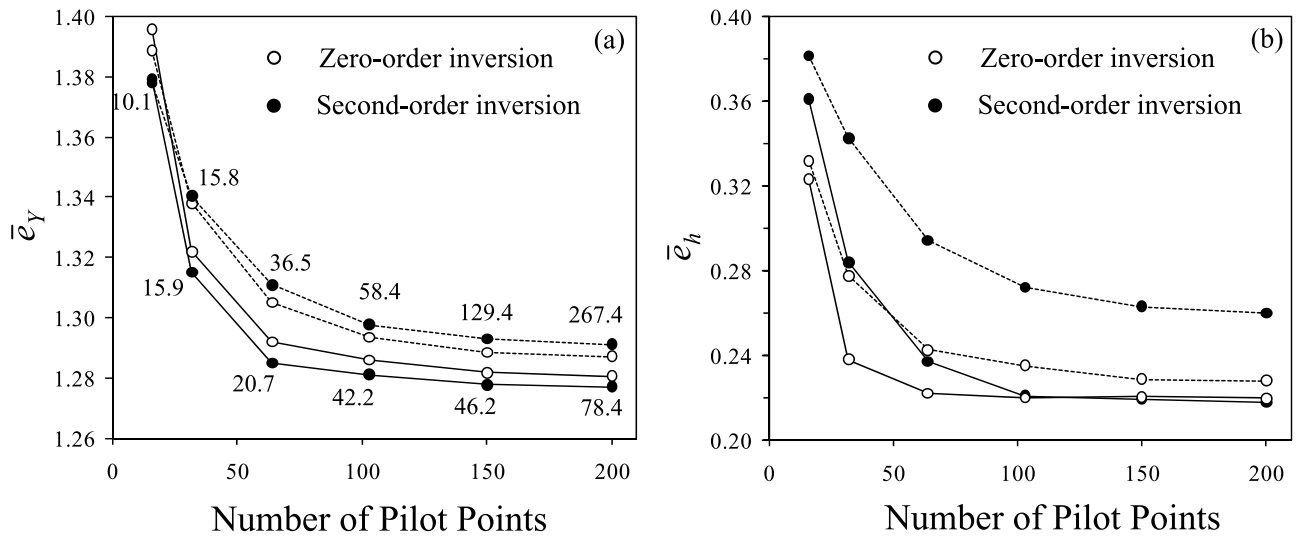


Figure 2. Mean absolute error of (a) Y , \bar{e}_Y , and (b) h , \bar{e}_h versus the number of pilot points obtained with zero- and second-order inversion with the reference values of $\sigma_Y^2 = 4.0$, $I_Y = 1.0$, and $\mu = 1.0$ evaluated with the exact sensitivity matrix (solid lines) and approximating the sensitivity matrix by the incremental ratio (dashed lines). Corresponding CPU times (in hours) are plotted next to the symbols.

that the inversion of moment equations is practically unaffordable for large values of model parameters without the direct evaluation of the sensitivity matrix. The superior accuracy of the exact derivatives reduces the number of Levenberg-Marquardt iterations. This, in addition to the fact that the system matrices needed to calculate the elements of the sensitivity matrix are identical for all the parameters (and coincide with those used to solve the state equations), leads to the observed drastic reduction of the computational load.

[23] As expected, \bar{e}_Y and \bar{e}_h decrease as the number of pilot points increases, regardless of the methodology used. We note that \bar{e}_Y and \bar{e}_h display a steep rate of decrease when N_p increases from 16 to 64. Further increments of N_p only result in marginal additional reductions of \bar{e}_Y and \bar{e}_h . A similar behavior has been obtained for various combinations of the statistical parameters (i.e., σ_Y^2 , I_Y and μ), albeit the value of N_p needed to obtain a plateau in \bar{e}_Y tends to slightly increase as σ_Y^2 , I_Y and μ decrease (not reported). This behavior is consistent with that observed by *Alcolea et al.* [2006a]. In their work, the authors were concerned with the geostatistical inversion of the traditional deterministic groundwater flow equation under the assumption that the parameters of the variogram of Y are known. A close inspection of *Alcolea et al.* [2006a, Figure 4], presenting the dependence of (24) on the regularization weight and 4 different values of N_p , reveals a behavior which is consistent with our zero-order inversion in Figure 2, for all values of the regularization weight tested by the authors. In our computational example, we note that when the exact sensitivity matrix is computed, the mean absolute error of Y is slightly smaller for the second-order than for the zero-order inversion while the mean absolute errors of h computed with zero- and second-order inversion are practically identical if N_p is sufficiently large.

[24] Additional analyses performed in terms of the model selection criteria defined in section 3 is not conducive to identify an optimum number of pilot points as all of them increase monotonically with N_p . A similar conclusion was

reached by *Alcolea et al.* [2006a], albeit in the context of deterministic inversion of groundwater flow. The authors noted that an appropriate identification of the optimum number of pilot points can be performed on the basis of criteria such as (24) and (25). Incidentally, we also note that the revised notion of KIC proposed by *Ye et al.* [2008, equation (14)], which has an expression equal to that included in (12) in which the term $N_Y \ln(N_Z)$ is subtracted, has the same qualitative behavior of (12) for our numerical example.

[25] With reference to the plausibility weight, our analysis reveals that NLL, AIC, AICc, HIC, and BIC are not conducive to the identification of an optimum value of μ , because they monotonically decrease with μ regardless of (1) the number of pilot points, (2) the values of σ_Y^2 and I_Y and (3) the order of inversion adopted. We found that the ability of KIC to identify the true plausibility weight increases with N_p and with the order of inversion regardless of the values of σ_Y^2 and I_Y adopted. Figure 3 reports the relative fraction of inversion runs for which KIC identifies a given value of μ as best, for different values of N_p and for all the tested combinations of σ_Y^2 and I_Y , both for zero- and second-order inversions. When a second-order inversion is used with $N_p \geq 32$, more than 90% of the test cases performed identify the optimum μ in the range [0.5, 1.0], the most frequent value being 0.5. This percentage slightly decreases when a zero-order inversion is performed. As shown in Figure 3, the adoption of a second-order inversion allows to exclude values of μ which are either much larger (≥ 5) or smaller (≤ 0.1) than the true, reference value. This notwithstanding, the ability of the zero-order inversion to identify the optimum value of the plausibility weight can be judged as satisfactory even with a relative small number of pilot points.

[26] We now ask how accurately can one estimate θ by means of geostatistical inversion of steady state stochastic moment equations of flow. Regardless of the number of pilot points, NLL (as well as AIC, AICc, HIC, and BIC) cannot identify the parameters of the variogram of Y ; it

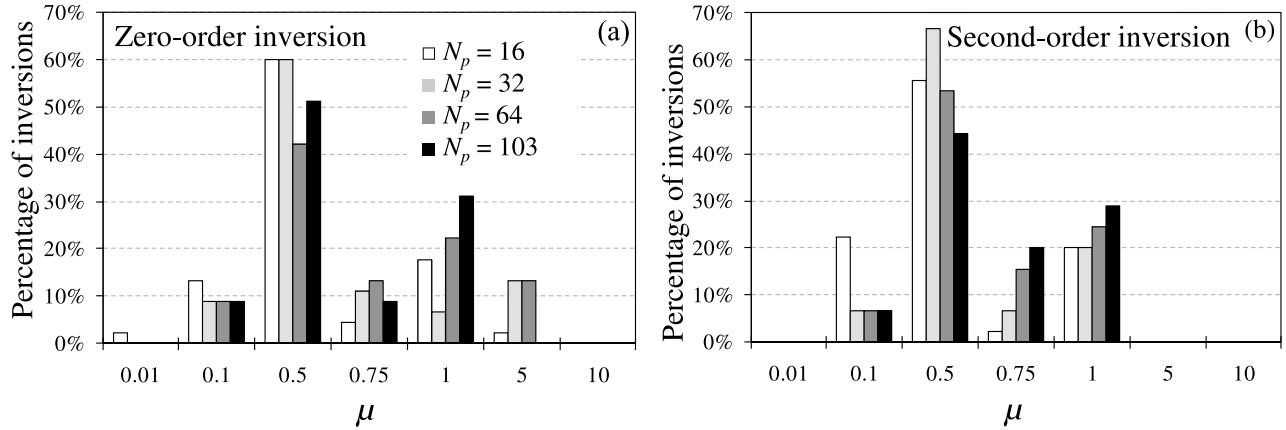


Figure 3. Relative fraction of (a) zero-order and (b) second-order inversions for which KIC identifies a given value of μ as best, for different values of N_p , and for all the analyzed combinations of σ_Y^2 and I_Y .

decreases as σ_Y^2 decreases for each combination of μ and I_Y . Figure 4 reports the relative fraction of inversions for which KIC identifies a given value of I_Y as best, for different values of N_p and for all combinations of σ_Y^2 and μ , both for zero- and second-order solutions. When a zero-order inversion is performed, $I_Y = 1.0$ is identified as the optimum value for about 60% of the test cases. This percentage slightly decreases to 50% when a second-order inversion is performed. Figure 5 shows the subset of the results included in Figure 4 corresponding to $0.5 \leq \mu \leq 1.0$; that is, the interval of μ values classified as best according to the analyses shown in Figure 3. It can be seen that in this case the relative fraction of inversions identifying the true reference value $I_Y = 1.0$ increases up to 100% when an adequate number of pilot points is adopted, regardless of the order of inversion.

[27] Finally, Table 1 reports the optimum values of μ (together with σ_{hE}^2 and σ_{YE}^2), σ_Y^2 and I_Y corresponding to the minimum of KIC obtained on the basis of zero- and second-order inversions for various values of N_p . Regardless of the order of inversion and the number of pilot points adopted, KIC identifies $\mu = 0.5$ and $I_Y = 1.0$ as best values. When a limited number of pilot points is used ($N_p = 32$), KIC on the basis of the second-order inversion correctly identifies

the true value of σ_Y^2 ($= 4.0$), while a zero-order inversion slightly overestimates it. When the number of pilot points increases, both zero- and second-order solutions tend to underestimate σ_Y^2 . This is consistent with our earlier observation that the use of a large number of pilot points does not necessarily renders a more accurate identification of all the parameters of interest.

[28] Table 2 reports a similar analysis performed when μ is considered to be known (e.g., when the experimental data are enough to support such an assumption) and set equal to 1.0 (the true, reference value in our test case). Again, KIC indicates as best the true value $I_Y = 1.0$, regardless of the order of inversion and N_p . The second-order inversion correctly identifies the true value of the sill almost for all values of N_p , even though it tends to slightly underestimate it when $N_p = 103$. The zero-order inversion significantly overestimates σ_Y^2 for small N_p values and renders results which are similar to those of a second-order inversion for increasing N_p .

[29] These results are also corroborated by Figure 6, where KIC is plotted as a function of σ_Y^2 for $I_Y = 1.0$, $\mu = 0.5$, 1.0 and various values of N_p . The difference between KIC obtained during a zero-order (dashed lines) and a second-

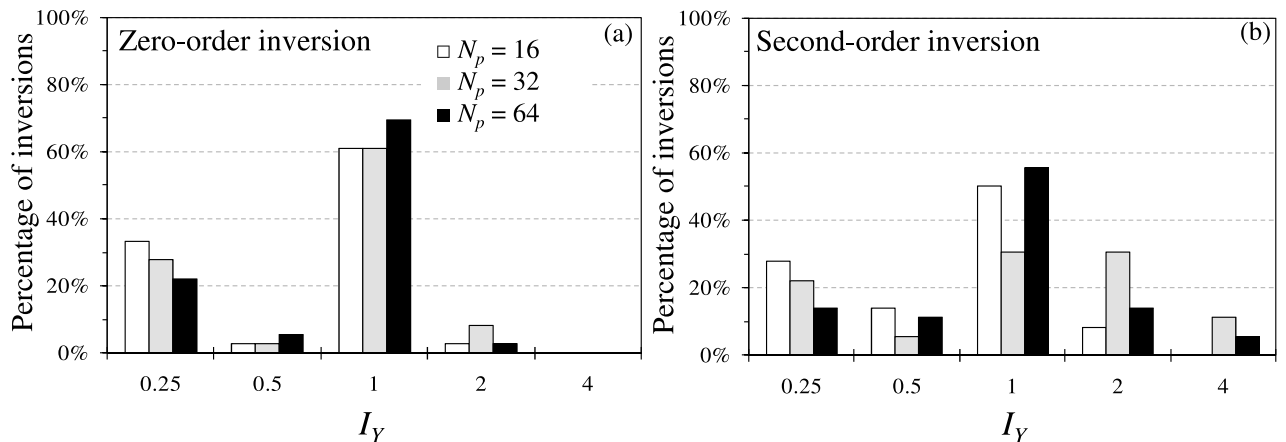


Figure 4. Relative fraction of (a) zero-order and (b) second-order inversions for which KIC identifies a given value of I_Y as best, for different values of N_p , and for all the analyzed combinations of σ_Y^2 and μ .

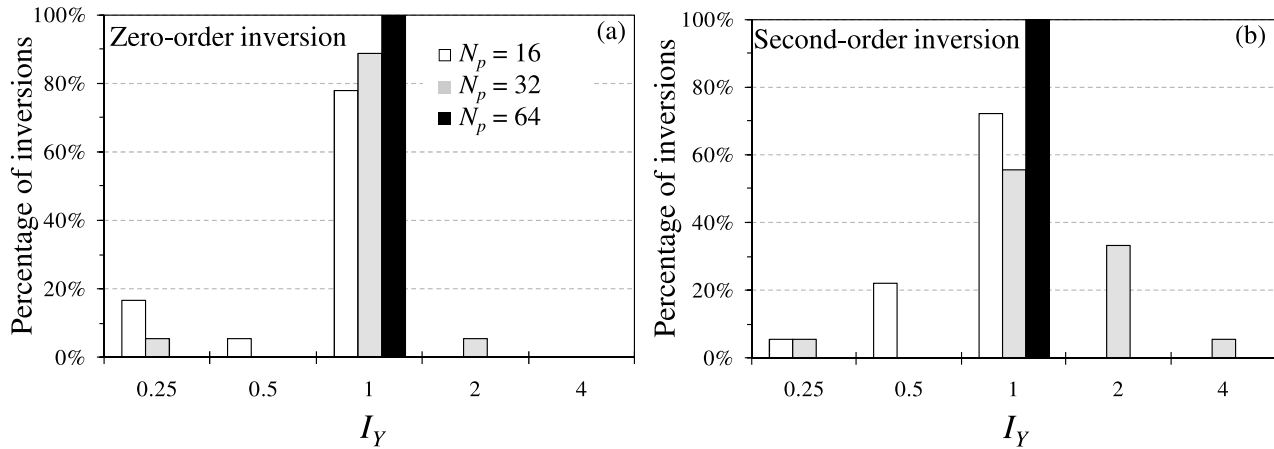


Figure 5. Relative fraction of (a) zero-order and (b) second-order inversions for which KIC identifies a given value of I_Y as best, for different values of N_p , and all tested values of σ_Y^2 when $0.5 \leq \mu \leq 1.0$.

order (solid lines) inversion tends to increase with σ_Y^2 and to decrease with N_p . When a limited number of pilot points is used, the second-order solution can identify the optimum sill more sharply than its zero-order counterpart.

[30] Finally, we note that our results indicate that the adoption of large values of N_p clearly underestimates the measurements errors σ_{hE}^2 and σ_{YE}^2 , estimated by (13). This is consistent with the observation of Neuman [1973] that, in the presence of data associated with measurement errors, the adoption of a number of parameters which is too large tends to allow fitting the model to noise, thus causing the quality of the parameter estimates to start deteriorating.

[31] Our results suggest that the geostatistical inversion of groundwater flow moment equations can lead to robust and computationally affordable estimates of hydraulic and statistical parameters (including the number of pilot points, the plausibility weight, σ_Y^2 and I_Y) of the system on the basis of successive inversions of zero- and second-order equations. The latter can be performed according to the procedure described in the following.

[32] 1. Perform a zero-order inversion for a set of cases designed upon varying μ , N_p , σ_Y^2 and I_Y (within a physically reasonable interval) and evaluate KIC. Find the value of μ that minimizes KIC for each combination of N_p , σ_Y^2 and I_Y .

[33] 2. Determine the optimum value of μ , $\bar{\mu}$, as the most frequent value of μ identified at step (1).

[34] 3. For the subset of simulations corresponding to $\mu = \bar{\mu}$, determine the value of I_Y that minimizes KIC for given combinations of N_p and σ_Y^2 .

[35] 4. Determine the optimum value of I_Y , \bar{I}_Y , as the most frequent value of I_Y identified at step (3).

Table 1. Best Estimates of μ , σ_{hE}^2 , σ_{YE}^2 , σ_Y^2 , and I_Y , Corresponding to the Minimum of KIC for Different Values of N_p

N_p	Zero-Order Inversion					Second-Order Inversion				
	μ	σ_Y^2	I_Y	σ_{hE}^2	σ_{YE}^2	μ	σ_Y^2	I_Y	σ_{hE}^2	σ_{YE}^2
16	0.5	4.0	1.0	0.7	1.4	0.5	3.0	1.0	0.7	1.5
32	0.5	4.5	1.0	0.5	1.0	0.5	4.0	1.0	0.5	1.1
64	0.5	3.0	1.0	0.4	0.7	0.5	3.0	1.0	0.4	0.7
103	0.5	2.0	1.0	0.3	0.5	0.5	2.0	1.0	0.3	0.6

[36] 5. Perform a set of second-order inversions with $\mu = \bar{\mu}$ and $I_Y = \bar{I}_Y$ for different combinations of N_p and σ_Y^2 and evaluate KIC.

[37] 6. Determine σ_Y^2 that minimize KIC evaluated at point (5) for various N_p . When a sufficiently large number of pilot points is used, the optimum value of σ_Y^2 , $\bar{\sigma}_Y^2$, is independent of N_p . When N_p becomes so large that the model starts being fitted to noise, a decrease of the estimated sill value is noted with N_p .

5.2. Variance of Log Conductivity and Hydraulic Head

[38] Following convergence of the minimization process, estimates of $Y(\mathbf{x})$ computed by (1) at element centroids, and corresponding variance-covariance values evaluated according to (9) are fully conditioned on all available data (log conductivity and heads). Thus, one can calculate the corresponding second-order conditional variance-covariance of predicted heads and fluxes (see equations (40)–(45) in the work of Guadagnini and Neuman [1999a]). These are fully conditioned on the same data. As an example, Figure 7 shows how the second-order conditional variance of Y , $Var_{Yc}^{[2]}(\mathbf{x})$, (Figure 7a) and of h , $Var_{hc}^{[2]}(\mathbf{x})$, (Figure 7b) varies along the cross section at $x_2 = 4.0$ (passing through the pumping well) when $\sigma_Y^2 = 4.0$, $I_Y = 1.0$ and $\mu = 1$. Figure 7 reports the results obtained with different numbers of pilot points and with the zero-order (dashed lines) and second-order (solid lines) inversions. The estimated variance of Y is practically insensitive to the order of the inversion of mean flow. It decreases as N_p increases, especially in the vicinity of the pilot points locations. A similar behavior is shown by the variance of the

Table 2. Best Estimates of σ_Y^2 , I_Y , and σ_{hE}^2 for Different Values of N_p and $\mu = 1$

N_p	Zero-Order Inversion			Second-Order Inversion		
	σ_Y^2	I_Y	σ_{hE}^2 ^a	σ_Y^2	I_Y	σ_{hE}^2 ^a
16	6.0	1.0	0.7	4.0	1.0	0.8
32	6.0	1.0	0.5	5.0	1.0	0.6
64	4.5	1.0	0.4	4.0	1.0	0.4
103	3.5	1.0	0.3	3.5	1.0	0.3

^aEqual to σ_{YE}^2 .

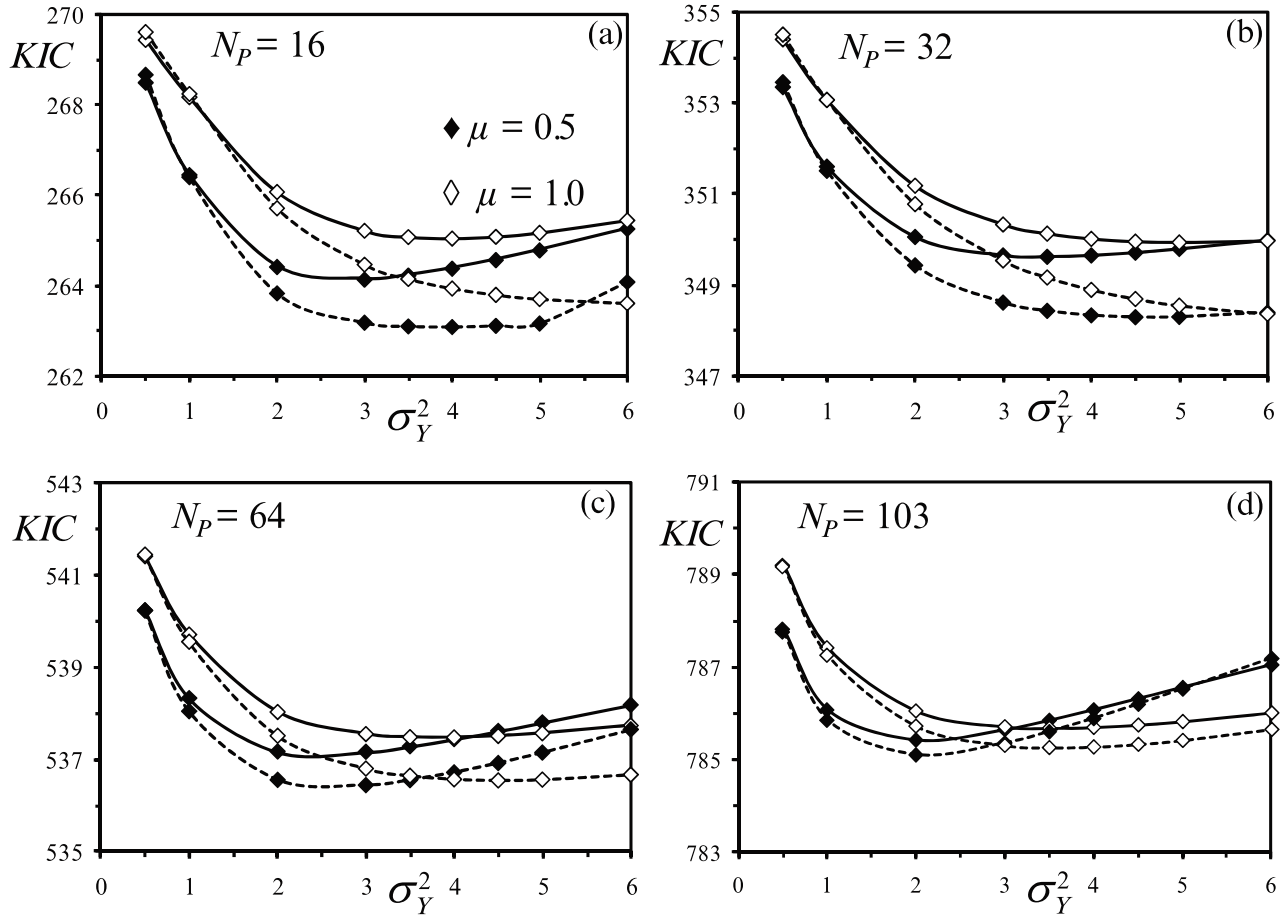


Figure 6. Dependence of KIC on σ_Y^2 obtained with zero-order (dashed curves) and second-order (continuous curves) inversions for $I_Y = 1.0$, $\mu = 0.5, 1.0$, and (a) $N_p = 16$, (b) $N_p = 32$, (c) $N_p = 64$, and (d) $N_p = 103$.

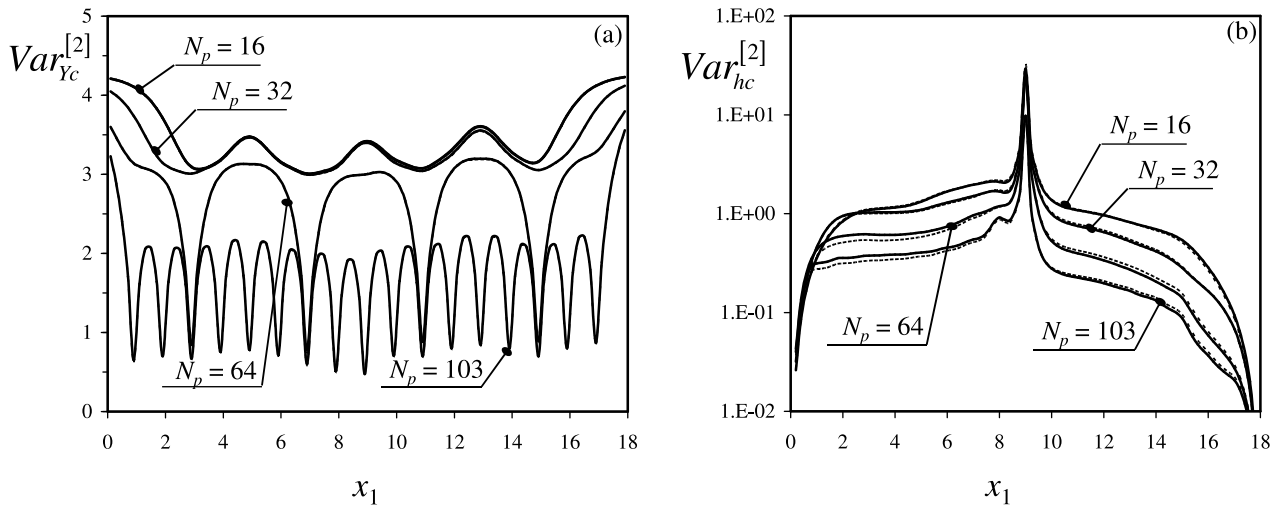


Figure 7. Cross sections at $x_2 = 4.0$ of the conditional (a) Y variance, $Var_{Yc}^{[2]}(\mathbf{x})$, and (b) h variance, $Var_{hc}^{[2]}(\mathbf{x})$, as function of N_p when $\sigma_Y^2 = 4.0$, $I_Y = 1.0$, and $\mu = 1$. The results of the zero- and the second-order inversion are depicted by dashed and continuous lines, respectively.

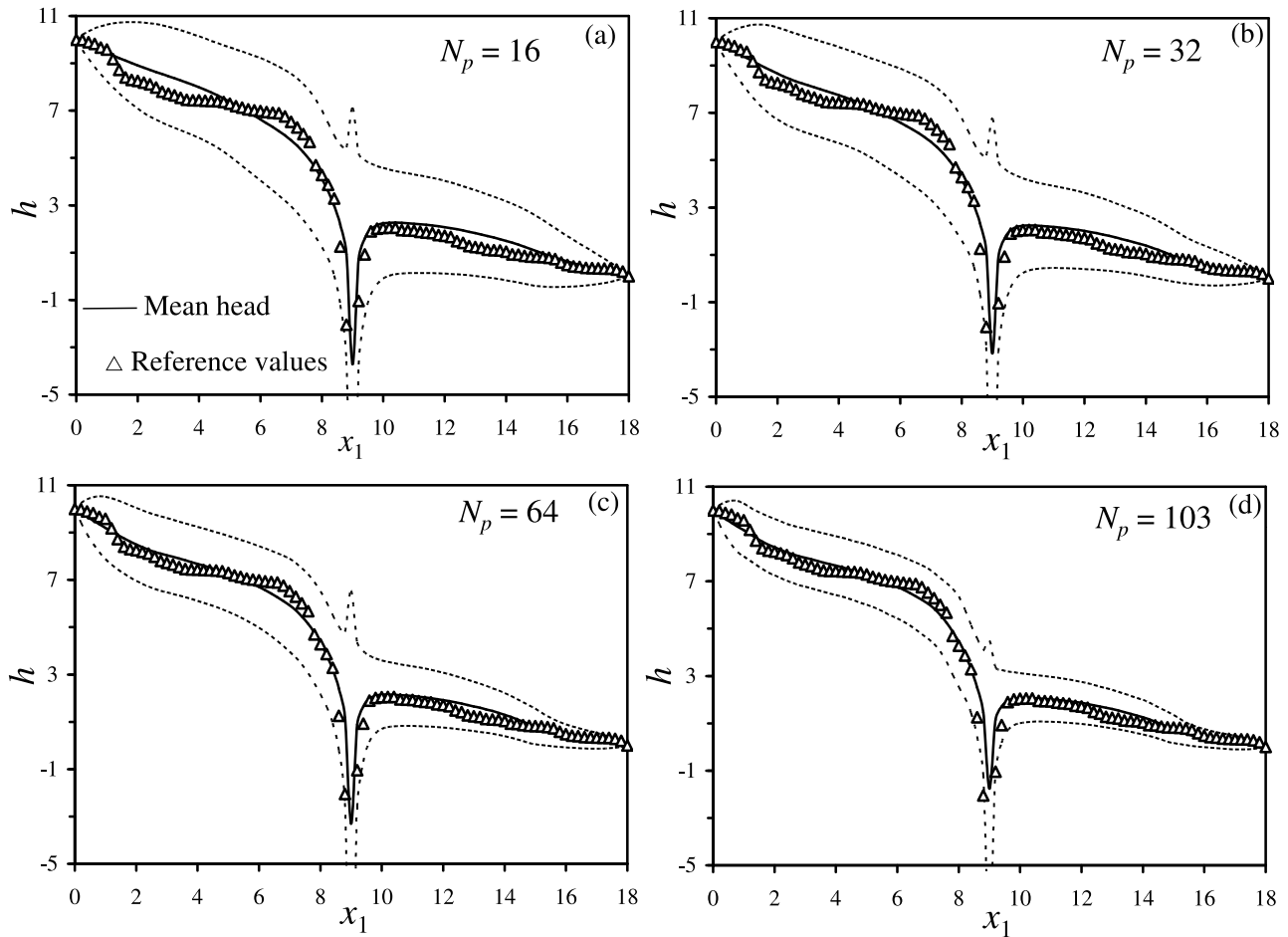


Figure 8. Cross sections at $x_2 = 4.0$ of the conditional mean head as function of N_p when $\sigma_Y^2 = 4.0$, $I_Y = 1.0$, and $\mu = 1$. Intervals corresponding to plus and minus two standard deviations of head estimates about the mean are also shown (dashed lines) together with hydraulic head reference values (symbols).

hydraulic head (Figure 7b) even though a larger effect of the order of the inversion is detectable. As a remark to these results, we note that prior estimates at pilot points locations are essentially treated as measurements (with associated inherent uncertainty) during inversion in the context of the Regularized Pilot Points Method [Alcolea *et al.*, 2006a; Hernandez *et al.*, 2006]. These prior values are estimated from available Y measurements and on the basis of a geostatistical model; the corresponding weight in the covariance matrix indicates how reliable they can be considered. In addition to this, we note that unknown Y values at pilot points are estimated on the basis of a nonlinear combination of Y and h at measurement points. It is therefore difficult to separate the effects of Y and h measurements on pilot points estimation variance so that, in principle, one cannot draw general conclusions by observing Figure 7. In this sense, as an alternative to a regular grid of pilot points (the location of which is fixed), one could consider exploring the effect of randomly varying the location of pilot points during the optimization process [Hendricks Franssen, 2001]. We do not pursue this point further in this work.

[39] Figure 8 displays a cross section (passing through the pumping well, at $x_2 = 4.0$) of the mean head obtained by

second-order inversion for different values of N_p and adopting the reference values for μ , σ_Y^2 and I_Y . Corresponding envelopes of $\pm 2\sqrt{\text{Var}_{hc}^{[2]}}$ (second-order standard deviation of heads) are also reported together with the reference head values. The mean hydraulic head is almost insensitive to N_p , and satisfactorily reproduces the reference head values. These always lay well within the envelopes depicted by the confidence intervals.

6. Conclusions

[40] We derived novel equations satisfied by the components of the sensitivity matrix of the (ensemble) mean hydraulic head (up to its second-order of approximation in σ_Y). The resulting system of equations has been solved by finite elements and embedded in an inverse procedure to condition recursive approximations of nonlocal ensemble moment equations of steady state flow jointly on measurements of log conductivity, Y , and hydraulic head, h . An advantage of this methodology is that the system matrices are identical for all the parameters and coincide with those used to solve the equations of the forward problem. Solving directly the aforementioned equations leads to a more accu-

rate reconstruction of the Y field (especially when a second-order inversion is performed) and to a considerable saving of the CPU time required to calculate the sensitivity matrix, as compared to other methods that approximate the sensitivity matrix by incremental ratios. At the same time, this allows the modeler to use a large number of unknown model parameters. We illustrate our algorithm and procedure by means of the synthetic example presented by *Hernandez et al.* [2006]. Our work leads to the following key results:

[41] 1. The mean absolute error between the reconstructed and true Y fields, $\bar{\epsilon}_Y$, tends to be slightly smaller for a second-order than for a zero-order inversion. Values of $\bar{\epsilon}_Y$ tend to decrease when the number of pilot points, N_p , increases, until they reach a plateau which is practically insensitive to N_p .

[42] 2. Identification criteria based on NLL, AIC, AICc, HIC, and BIC are in general not conducive to the identification of an optimum value of the plausibility weight and variogram parameters.

[43] 3. Estimation of the plausibility weight and integral scale of Y is quite robust and can be performed with a limited number of pilot points and with a low-order approximation of the moment equations. The latter coincides with the solution of the traditional deterministic flow equation in an aquifer with local hydraulic conductivity equal to the mean geometric hydraulic conductivity, $K_G(\mathbf{x})$. The ability of KIC to identify μ tends to increase with N_p and (slightly) with the order of inversion, regardless of the assumed statistical parameters of the underlying Y field.

[44] 4. When a limited number of pilot points is used, the second-order solution can identify the optimum sill more sharply than its zero-order counterpart. When N_p becomes so large that the model starts being fitted to noise, a decrease of the estimated sill value is noted with N_p . When a sufficiently reliable estimate of μ is available (e.g., when experimental information can support such an assumption) the ability of the second-order inversion to correctly identify the true value of σ_Y^2 increases.

[45] 5. In our setting and for the chosen arrangement of pilot points, we found that the posterior variance of Y and h tends to decrease as the number of pilot points increases, especially in the vicinity of Y measurement and pilot points locations.

[46] 6. On the basis of our computational example, one can see that the use of a large number of pilot points does not necessarily imply a more accurate identification of all the parameters of interest. At the same time, the number of pilot points should be large enough to provide the characterization of the Y field with enough degrees of freedom. However, a very large number of model parameters tends to favor noise fitting, thus causing a deterioration of the quality of parameter estimates. The optimum number of pilot points to be adopted during inversion of moment equations of groundwater flow depends on the quantity one desires to determine (i.e., the spatial distribution of mean Y , the parameters of the Y variogram, the measurement error associated with the experimental data) and on the adopted flow model (zero- or second-order equations). Our example indicates that one should gradually increase N_p until the desired quantities become insensitive to it.

[47] 7. Our results suggest that the geostatistical inversion of groundwater flow moment equations can benefit from successive inversions of zero- and second-order equations to provide a robust and computationally affordable estimate

of hydraulic and (geo-)statistical parameters (including the number of pilot points) of the problem. In principle our approach can be extended to accommodate a conceptualization of a heterogeneous porous domain as a composite medium, whenever the latter is embedded in the context of groundwater flow moment equations, as proposed by *Winter and Tartakovsky* [2000, 2002] and *Winter et al.* [2002]. It is also amenable to incorporate a multiscale description of heterogeneous transmissivity, whenever the latter can be depicted by means of a truncated power variogram, in the spirit of *Neuman and Di Federico* [2003, and references therein] and *Neuman et al.* [2008].

Appendix A: Finite Element Equations for Mean Hydraulic Head

[48] We consider steady state flow of groundwater in a randomly heterogeneous flow domain, Ω . The flux vector $\mathbf{q}(\mathbf{x})$ and the hydraulic head $h(\mathbf{x})$ obey the continuity equation and Darcy's Law subject to given forcing terms (sources and boundary conditions). Optimum unbiased predictions of $h(\mathbf{x})$ and $\mathbf{q}(\mathbf{x})$ can be rendered via their first ensemble (statistical) moments (expected or mean values), $\langle h(\mathbf{x}) \rangle_c$ and $\langle \mathbf{q}(\mathbf{x}) \rangle_c$. Exact integrodifferential equations for $\langle h(\mathbf{x}) \rangle_c$ and $\langle \mathbf{q}(\mathbf{x}) \rangle_c$ and the conditional second-moment (variance-covariance) of associated head and flux prediction errors can be found in the work of *Guadagnini and Neuman* [1999a]. *Guadagnini and Neuman* [1999b] then solve the equations satisfied by the zero- and second-order components of mean and variance-covariance of hydraulic head by a Galerkin finite element scheme in a two-dimensional rectangular domain, in the presence of deterministic forcing terms. In the following we report only the results of *Guadagnini and Neuman* [1999a] that are necessary for the derivation of the sensitivity matrix for mean heads presented in section 4.

[49] The zero-order finite element equations for the mean hydraulic heads read

$$\sum_{m=1}^N A_{nm} h_m^{(0)} = b_{0n}; \quad n = 1, 2, \dots, N \quad (\text{A1})$$

Here, $h_m^{(0)} \equiv \langle h^{(0)}(\mathbf{x}_m) \rangle_c$ is the zero-order approximation of the mean hydraulic head, N the number of nodes in the numerical mesh, excluding those on Dirichlet boundary, Γ_D , b_{0n} is a mean forcing term at node n and A_{nm} are the terms of a sparse, symmetric matrix given by

$$A_{nm} = \int_{\Omega} K_G(\mathbf{x}) \nabla \psi_n(\mathbf{x}) \bullet \nabla \psi_m(\mathbf{x}) d\mathbf{x} \quad (\text{A2})$$

$K_G(\mathbf{x}) = \exp \langle Y(\mathbf{x}) \rangle_c$ and $\psi_n(\mathbf{x})$ are bilinear basis functions.

[50] The corresponding second-order finite element equations are

$$\sum_{m=1}^N [A_{nm} h_m^{(2)} + B_{nm} h_m^{(0)}] = P_n + S_n; \quad n = 1, 2, \dots, N \quad (\text{A3})$$

where $h_m^{(2)} \equiv \langle h^{(2)}(\mathbf{x}) \rangle_c$ is a second-order correction to $h_m^{(0)}$, their sum yielding the second-order approximation of the mean hydraulic head

$$\langle h_m^{[2]} \rangle_c = h_m^{(0)} + h_m^{(2)} \quad (\text{A4})$$

B_{nm} are terms of a sparse, symmetric matrix given by

$$B_{nm} = \frac{1}{2} \int_{\Omega} K_G(\mathbf{x}) \sigma_Y^2(\mathbf{x}) \nabla \psi_n(\mathbf{x}) \bullet \nabla \psi_m(\mathbf{x}) d\mathbf{x} \quad (\text{A5})$$

The coefficients P_n and S_n are computed according to

$$P_n = - \sum_{m=1}^{N_D} [A_{nm} h_m^{(2)} + B_{nm} h_m^{(0)}] \quad (\text{A6})$$

$$S_n = \sum_{e=1}^{M_x} K_G(e) \sum_{i=1}^{N_x} \theta_{ni}^{ee} \sum_{e'=1}^{M_y} K_G(e') \langle Y'(e) Y'(e') \rangle_c \cdot \sum_{l=1}^{N_y} G_{il}^{ee'} \sum_{k=1}^{N_x} h_k^{(0)e'} \Delta_{lk}^{e'e'} \quad (\text{A7})$$

where N_D is the number of nodes on Γ_D , M_x and M_y are number of elements in \mathbf{x} and \mathbf{y} planes, respectively; $K_G(e)$ is the (uniform) value of $K_G(\mathbf{x})$ in element e ; N_x and N_y are the number of nodes in element e and e' within the \mathbf{x} and \mathbf{y} planes, respectively; $\langle Y'(e) Y'(e') \rangle_c$ is the conditional covariance between $Y'(e) = Y(e) - \langle Y(e) \rangle_c$ in element e and $Y'(e')$ in element e' , the covariance being calculated between the elements centers of gravity; $G_{il}^{ee'}$ is the Green's function associated with the zero-order mean flow equation (A1) evaluated at node i of element e owing to a unit source at node l of element e' (see Appendix B); $h_k^{(0)e'}$ is zero-order head at node k of element e' in the \mathbf{y} plane; θ_{ni}^{ee} and $\Delta_{lk}^{e'e'}$ are defined as:

$$\theta_{ni}^{ee} = \int_e \nabla_x \psi_n(\mathbf{x}^e) \bullet \nabla_x \psi_i(\mathbf{x}^e) d\mathbf{x} \quad (\text{A8})$$

$$\Delta_{lk}^{e'e'} = \int_{e'} \nabla_y \psi_j(\mathbf{y}^{e'}) \bullet \nabla_y \psi_k(\mathbf{y}^{e'}) d\mathbf{y} \quad (\text{A9})$$

with the integrals being computed over elements e and e' .

Appendix B: Finite Element Equations for the Zero-Order Green's Function and Its Derivatives With Respect to Model Parameters

[51] The zero-order approximation of the mean Green's function satisfies [Guadagnini and Neuman, 1999a]

$$\nabla_y [K_G(\mathbf{y}) \nabla_y \langle G^{(0)}(\mathbf{y}, \mathbf{x}) \rangle_c] + \delta(\mathbf{y} - \mathbf{x}) = 0; \text{ on } \Omega \quad (\text{B1})$$

with homogeneous boundary conditions. Equation (B1) is solved by finite elements upon placing a point source of unit strength at node p ($p = 1, 2, \dots, N$) in the \mathbf{x} plane according to

$$\sum_{m=1}^N A_{nm} G_{mp} = -1 \quad n = 1, 2, \dots, N \quad (\text{B2})$$

Making use of (16) and (17), the derivative of the order approximation of the mean Green's function with respect to the j th hydraulic parameter Y_{H_j} ($j = 1, \dots, N_Y$) is given by

$$\sum_{m=1}^N A_{nm} \frac{\partial G_{mp}}{\partial Y_{H_j}} = - \sum_{m=1}^N G_{mp} \left(\int_{\Omega} \exp \langle Y(\mathbf{x}) \rangle_c \lambda_j(\mathbf{x}) \nabla \psi_n \bullet \nabla \psi_m d\mathbf{x} \right) \quad (\text{B3})$$

[52] **Acknowledgments.** We thank Shlomo P. Neuman of the University of Arizona for his thoughtful comments and suggestions. The work has been partly supported by the Marie Curie Initial Training Network's Towards Improved Groundwater Vulnerability Assessment (IMVUL). Additional funding from the Politecnico di Milano (Project GEMINO, Progetti di ricerca 5 per mille junior) is acknowledged.

References

- Akaike, H. (1974), A new look at statistical model identification, *IEEE Trans. Autom. Control*, *19*, 716–723, doi:10.1109/TAC.1974.1100705.
- Alcolea, A., J. Carrera, and A. Medina (2006a), Pilot points method incorporating prior information for solving the groundwater flow inverse problem, *Adv. Water Resour.*, *29*, 1678–1689, doi:10.1016/j.advwatres.2005.12.009.
- Alcolea, A., J. Carrera, and A. Medina (2006b), Inversion of heterogeneous parabolic-type equations using the pilot points method, *Int. J. Numer. Methods Fluids*, *51*, 963–980, doi:10.1002/flid.1213.
- Capilla, J. E., J. J. Gómez-Hernández, and A. Sahuquillo (1997), Stochastic simulation of transmissivity fields conditional to both transmissivity and piezometric head data—2. Demonstration on a synthetic aquifer, *J. Hydrol. Amsterdam*, *203*, 175–188, doi:10.1016/S0022-1694(97)00097-8.
- Carrera, J., and S. P. Neuman (1986a), Estimation of aquifer parameters under transient and steady state conditions: 1. Maximum likelihood method incorporating prior information, *Water Resour. Res.*, *22*, 199–210, doi:10.1029/WR022i002p00199.
- Carrera, J., and S. P. Neuman (1986b), Estimation of aquifer parameters under transient and steady state conditions: 2. Uniqueness, stability, and solution algorithms, *Water Resour. Res.*, *22*, 211–227, doi:10.1029/WR022i002p00211.
- Carrera, J., and S. P. Neuman (1986c), Estimation of aquifer parameters under transient and steady state conditions: 3. Application to synthetic and field data, *Water Resour. Res.*, *22*, 228–242, doi:10.1029/WR022i002p00228.
- Carrera, J., A. Alcolea, A. Medina, J. Hidalgo, and L. J. Slooten (2005), Inverse problem in hydrogeology, *Hydrogeol. J.*, *13*, 206–222, doi:10.1007/s10040-004-0404-7.
- Christensen, S., and J. Doherty (2008), Using many pilot points and singular value decomposition in groundwater model calibration, *IAHS Publ.*, *320*, 235–239.
- Cooley, R. L. (2000), An analysis of the pilot point methodology for automated calibration of an ensemble of conditionally simulated transmissivity fields, *Water Resour. Res.*, *36*, 1159–1163, doi:10.1029/2000WR900008.
- Dagan, G. (1985), Stochastic modeling of groundwater flow by unconditional and conditional probabilities: The inverse problem, *Water Resour. Res.*, *21*, 65–72, doi:10.1029/WR021i001p00065.
- Dagan, G., and S. P. Neuman (Eds.) (1997), *Subsurface Flow and Transport*, Cambridge Univ. Press, New York, doi:10.1017/CBO9780511600081.
- de Marsily, G. (1978) De l'identification des systemes hydrogeologiques, Ph.D. dissertation, Pierre and Marie Curie Univ., Paris.
- de Marsily, G., C. Lavedan, M. Bouchere, and G. Fasanino (1984), Interpretation of interference tests in a well field using geostatistical techniques to fit the permeability distribution in a reservoir model, in *Geostatistics for Natural Resources Characterization, Part 2, NATO ASI Ser., Ser. C*, vol. 182, edited by G. Verly et al., pp. 831–849, D. Reidel, Dordrecht, Holland.
- Deutsch, C. V., and A. G. Journel (1998), *GSLIB Geostatistical Software Library and User's Guide*, Oxford Univ. Press, New York.
- Doherty, J. (2002), *PEST: Model Independent Parameter Estimation, User Manual*, 4th ed., Watermark Numer. Comput. Corinda, Queensland.
- Gómez-Hernández, J. J., and A. G. Journel (1993), Joint sequential simulation of multi-Gaussian field, in *Geostatistics Troia '92*, vol. 1, edited by A. O. Soares, pp. 85–94, Springer, New York.
- Gómez-Hernández, J. J., A. Sahuquillo, and J. E. Capilla (1997), Stochastic simulation of transmissivity fields conditional to both transmissivity and piezometric data—1. Theory, *J. Hydrol. Amsterdam*, *203*, 162–174.
- Guadagnini, A., and S. P. Neuman (1999a), Nonlocal and localized analyses of conditional mean steady state flow in bounded, randomly nonuniform domains: 1. Theory and computational approach, *Water Resour. Res.*, *35*, 2999–3018, doi:10.1029/1999WR900160.
- Guadagnini, A., and S. P. Neuman (1999b), Nonlocal and localized analyses of conditional mean steady state flow in bounded, randomly nonuniform domains: 2. Computational examples, *Water Resour. Res.*, *35*, 3019–3039, doi:10.1029/1999WR900159.

- Guadagnini, A., M. Riva, and S. P. Neuman (2003), Three-dimensional steady state flow to a well in a randomly heterogeneous bounded aquifer, *Water Resour. Res.*, 39(3), 1048, doi:10.1029/2002WR001443.
- Gutjahr, A. L., and J. R. Wilson (1989), Co-kriging for stochastic flow models, *Transp. Porous Media*, 4, 585–598, doi:10.1007/BF00223629.
- Hanna, S., and T. C. J. Yeh (1998), Estimation of co-conditional moments of transmissivity, hydraulic head, and velocity fields, *Adv. Water Resour.*, 22, 87–95, doi:10.1016/S0309-1708(97)00033-X.
- Hannan, E. S. (1980), The estimation of the order of an ARMA process, *Ann. Stat.*, 8, 1071–1081, doi:10.1214/aos/1176345144.
- Hendricks Franssen, H. J. (2001), Inverse stochastic modeling of groundwater flow and mass transport, Ph.D. thesis, Tech. Univ. of Valencia, Valencia, Spain.
- Hendricks Franssen, H. J., and J. J. Gómez-Hernández (2002), 3D inverse modelling of groundwater flow at a fractured site using a stochastic continuum model with multiple statistical populations, *Stochastic Environ. Res. Risk Assess.*, 16, 155–174, doi:10.1007/s00477-002-0091-7.
- Hendricks Franssen, H. J., A. Alcolea, M. Riva, M. Bakr, N. van der Wiel, F. Stauffer, and A. Guadagnini (2009), A comparison of seven methods for the inverse modeling of groundwater flow: Application to the characterisation of well catchments, *Adv. Water Resour.*, 32, 851–872, doi:10.1016/j.advwatres.2009.02.011.
- Hernandez, A. F., S. P. Neuman, A. Guadagnini, and J. Carrera (2003), Conditioning mean steady state flow on hydraulic head and conductivity through geostatistical inversion, *Stochastic Environ. Res. Risk Assess.*, 17, 329–338, doi:10.1007/s00477-003-0154-4.
- Hernandez, A. F., S. P. Neuman, A. Guadagnini, and J. Carrera (2006), Inverse stochastic moment analysis of steady state flow in randomly heterogeneous media, *Water Resour. Res.*, 42, W05425, doi:10.1029/2005WR004449.
- Hoeksema, R. J., and P. K. Kitanidis (1984), An application of the geostatistical approach to the inverse problem in two-dimensional groundwater modeling, *Water Resour. Res.*, 20, 1003–1020, doi:10.1029/WR020i007p01003.
- Hurvich, C. M., and C. L. Tsai (1989), Regression and time series model selection in small sample, *Biometrika*, 76, 297–307, doi:10.1093/biomet/76.2.297.
- Jiang, Y., A. D. Woodbury, and S. Painter (2004), A full-Bayesian inversion of the Edwards Aquifer, *Ground Water*, 42, 724–733, doi:10.1111/j.1745-6584.2004.tb02726.x.
- Kashyap, R. L. (1982), Optimal choice of AR and MA parts in autoregressive moving average models, *IEEE Trans. Pattern Anal. Mach. Intel.*, 4, 99–104, doi:10.1109/TPAMI.1982.4767213.
- LaVenue, A. M., B. S. RamaRao, G. de Marsily, and M. G. Marietta (1995), Pilot point methodology for automated calibration of an ensemble of conditionally simulated transmissivity fields: 2. Application, *Water Resour. Res.*, 31, 495–516, doi:10.1029/94WR02259.
- LaVenue, M., and G. de Marsily (2001), Three-dimensional inference test interpretation in a fractured aquifer using the pilot point inverse method, *Water Resour. Res.*, 37, 2659–2675.
- Marquardt, D. W. (1963), An algorithm for least-squares estimation of nonlinear parameters, *SIAM J. Appl. Math.*, 11, 431–441, doi:10.1137/0111030.
- Medina, A., and J. Carrera (2003), Geostatistical inversion of coupled problems: Dealing with computational burden and different types of data, *J. Hydrol. Amsterdam*, 281, 251–264, doi:10.1016/S0022-1694(03)00190-2.
- Neuman, S. P. (1973), Calibration of distributed parameter groundwater flow models viewed as a multiple-objective decision process under uncertainty, *Water Resour. Res.*, 9, 1006–1021, doi:10.1029/WR009i004p01006.
- Neuman, S. P., and V. Di Federico (2003), Multifaceted nature of hydrogeologic scaling and its interpretation, *Rev. Geophys.*, 41(3), 1014, doi:10.1029/2003RG000130.
- Neuman, S. P., and A. Guadagnini (1999), A new look at traditional deterministic flow models and their calibration in the context of randomly heterogeneous media, *IAHS Publ.*, 26, 213–221.
- Neuman, S. P., and S. Orr (1993), Prediction of steady state flow in non-uniform geologic media by conditional moments: Exact nonlocal formalism, effective conductivities, and weak approximation, *Water Resour. Res.*, 29, 341–364, doi:10.1029/92WR02062.
- Neuman, S. P., M. Riva, and A. Guadagnini (2008), On the geostatistical characterization of hierarchical media, *Water Resour. Res.*, 44, W02403, doi:10.1029/2007WR006228.
- Nowak, W., and O. A. Cirpka (2004), A modified Levenberg-Marquardt algorithm for quasi-linear geostatistical inverting, *Adv. Water Resour.*, 27, 737–750, doi:10.1016/j.advwatres.2004.03.004.
- Oliver, D. S., L. B. Cunha, and A. C. Reynolds (1997), Markov chain Monte Carlo methods for conditioning a permeability field to pressure data, *Math. Geol.*, 29, 61–91, doi:10.1007/BF02769620.
- RamaRao, B. S., A. M. LaVenue, G. de Marsily, and M. G. Marietta (1995), Pilot point methodology for automated calibration of an ensemble of conditionally simulated transmissivity fields: 1. Theory and computational experiments, *Water Resour. Res.*, 31, 475–493, doi:10.1029/94WR02258.
- Riva, M., A. Guadagnini, S. P. Neuman, and S. Franzetti (2001), Radial flow in a bounded, randomly heterogeneous aquifer, *Transp. Porous Media*, 45, 139–193, doi:10.1023/A:1011880602668.
- Rubin, Y., and G. Dagan (1987), Stochastic identification of transmissivity and effective recharge in steady groundwater flow: 1. Theory, *Water Resour. Res.*, 23, 1185–1192, doi:10.1029/WR023i007p01185.
- Sahuquillo, A. J., E. Capilla, J. J. Gómez-Hernández, and J. Andreu (1992), Conditional simulation of transmissivity fields honoring piezometric data, in *Fluid Flow Modelling*, edited by W. R. Blain and E. Cabrera, pp. 201–212, Elsevier, London.
- Samper, F. J., and S. P. Neuman (1989a), Estimation of spatial covariance structures by adjoint state maximum likelihood cross validation: 1. Theory, *Water Resour. Res.*, 25, 351–362, doi:10.1029/WR025i003p00351.
- Samper, F. J., and S. P. Neuman (1989b), Estimation of spatial covariance structures by adjoint state maximum likelihood cross-validation: 2. Synthetic experiments, *Water Resour. Res.*, 25, 363–372, doi:10.1029/WR025i003p00363.
- Schwarz, G. (1978), Estimating the dimension of a model, *Ann. Stat.*, 6, 461–464, doi:10.1214/aos/1176344136.
- Tikhonov, A. N. (1963a), Regularization of incorrectly posed problems, *Sov. Math Dokl.*, 4, 1624–1627.
- Tikhonov, A. N. (1963b), Solution of incorrectly formulated problems and the regularization method, *Sov. Math Dokl.*, 4, 1035–1038.
- Winter, C. L., and D. M. Tartakovsky (2000), Mean flow in composite porous media, *Geophys. Res. Lett.*, 27, 1759–1762, doi:10.1029/1999GL011030.
- Winter, C. L., and D. M. Tartakovsky (2002), Groundwater flow in heterogeneous composite aquifers, *Water Resour. Res.*, 38(8), 1148, doi:10.1029/2001WR000450.
- Winter, C. L., D. M. Tartakovsky, and A. Guadagnini (2002), Numerical solutions of moment equations for flow in heterogeneous composite aquifers, *Water Resour. Res.*, 38(5), 1055, doi:10.1029/2001WR000222.
- Woodbury, A. D., and T. J. Ulrych (2000), A full-Bayesian approach to the groundwater inverse problem for steady state flow, *Water Resour. Res.*, 36, 2081–2093, doi:10.1029/2000WR900086.
- Ye, M., P. D. Meyer, and S. P. Neuman (2008), On model selection criteria in multimodel analysis, *Water Resour. Res.*, 44, W03428, doi:10.1029/2008WR006803.
- Zimmerman, D. A., et al. (1998), A comparison of seven geostatistically based inverse approaches to estimate transmissivities for modeling advective transport by groundwater flow, *Water Resour. Res.*, 34, 1373–1413, doi:10.1029/98WR00003.

A. Alcolea, TK Consult AG, Seefeldstrasse 287, CH-8008 Zürich, Switzerland.

F. De Gaspari, GHS, Department of Geotechnical Engineering and Geosciences, Universitat Politècnica de Catalunya, UPC-Barcelona Tech, Jordi Girona 1-3, E-08034 Barcelona, Spain.

A. Guadagnini and M. Riva, Dipartimento Ingegneria Idraulica, Ambientale, Infrastrutture Viarie, e Rilevamento, Politecnico di Milano, Piazza L. Da Vinci 32, I-20133 Milan, Italy. (monica.riva@polimi.it)